



MedCrave

Step into the World of Research



The Role of Pin1 in Controls Tumor Cell Proliferation in Mouse Lung Cancer Conditional Model

Daive De Carlo

The Role of Pin1 in Controls Tumor Cell Proliferation in Mouse Lung Cancer Conditional Model

ABOUT THE AUTHORS

**Davide De Carlo^{1*}, Marco Muzi Falconi², Antonio³
and Dott ssa Silvia Boffo⁴**

¹Department of Biosciences, University of Milan, Italy

²Reporter, Italy

³Coreporter, Italy

⁴Tutor, Italy

***Corresponding author:**

Davide De Carlo, Department of Biosciences, University of Milan, Italy Tel: +39.3407657495; Fax: +39.5520021555;
Email: decarlodavider@gmail.com

Published By:

MedCrave Group LLC

November 30, 2017

Contents

Abstract	1
Abbreviations	2
Introduction	3
Lung cancer	3
Tumor microenvironment	3
Molecular events associated to lung cancer	5
Lentiviral vectors	11
Lung cancer mouse conditional model	13
Aim of study	15
Materials and methods	18
Lung cancer conditional model	18
Genotyping mice (p53 and kras)	21
Lentivirus production and purification	23
Lentiviral titration methods	25
Histopathological analysis of lung cancer in mice	26
Results	26
Results lentiviral titration methods	27
The pathological diagnosis on mice model	29
Discussion	32
Common mutations in nslc	32
Conclusion	34
Acknowledgement	34
Conflict of Interest	34
References	34

Abstract

There are some pathways that are altered in many tumors, and RB and p53 pathways are two of the most important. These proteins are regulated during carcinogenesis by a phosphorylation mechanism. Ser or Thr followed by Pro are major phosphorylation motifs in the cells but their significance was obscure until the discovery of the PIN1 protein (protein interacting with NIMA (never in mitosis A)-1). Pin1 isomerase specific of pSer/Thr-Pro motifs that catalyzed the conformational switch from cis to Trans, which is especially important because Pro-directed kinases and phosphatases are conformation-specific and act only on the Trans conformation. In vivo and in vitro data have demonstrated that Pin1 is involved in many aspects of cell cycle control. We studied the role of Pin1 in controls tumor cell proliferation using a conditional mouse model. Our results show a marked increase of tumorigenesis and metastasis in mutated murine models. We produced lentivirus containing CRE, HAPIN1 and HAPIN1 S67E sequences and we used these viruses to infect mice's lungs, obtaining a lung cancer conditional model through Cre-Lox recombination method. Finally we characterized the effects induced by 4 different time points. For each time point we analyzed the histology characteristics of the induced lung cancer.

Keywords: Lung cancer; Prevalent cancer; Killer cancer; Large-cell carcinomas; Neuroendocrine cells; Bronchial tree; Gene-enzyme; Mucosal lymphatic vessels; Regional lymph nodes; Bronchial invasion; Phenotype; Epigenetic abnormalities; Disease prevention; metastasis; Epidermal growth factor receptor; Proto-oncogenes; Cell lung carcinomas; Tumor suppressor genes; Telomere length; Lung carcinogenesis hallmark of cancer; Cytotoxic; Myeloid-derived suppressor cells; Small-molecule inhibitors; DNA-binding domain; Regulatory pathway; Cells in culture; Kill cells; Tumorigenic potential

List of Abbreviation

TAM: Tumor Associated Macrophages

DC: Dendritic Cell

CTLs and Tregs: Cyto Toxic and Regulatory T-cells

NK: Natural Killer

MDSCs: Myeloid Derived Suppressor Cells

VEGF: Vascular Endothelial Growth Factor

GM-CSF: Granulocyte-Macrophage Colony-Stimulating Factor

NSCLC: Non-Small Cell Lung Cancer

SCLC: Small-Cell Lung Cancer

TSG: Tumor Suppressor Genes

GDP: Guanosine Di Phosphates

GTP: Guanosine Triphosphate

MLK: Mixed-Lineage Kinase

SENP: SUMO Protease

GRK2: G protein-coupled Receptor Kinase 2

CDK2: Cyclic- Dependent Kinase 2

ER α : Estrogen receptor- α

SMRT: Silencing Mediator for Retinoic Acid and Thyroid Hormone Receptor

FOXO: Forehead Box O

PML: Promyelocytic Leukemia Protein

RUNX3: Runt-Related Transcription Factor 3

TGF- β : Transforming Growth Factor- β

CDKs: Cyclic-Dependent Protein Kinases

MAPKs: Mitogen-Activated Protein Kinases

ERKs: Extracellular Signal- Regulated Kinases

SAPKs/JNKs: Stress-Activated Protein Kinases/C-Jun N-Terminal Kinases

GSK3: Glycogen Synthase Kinase 3

PLKs: Polo-Like Kinases PPlase: Peptide *polyol cis/transisomerases*

Introduction

Lung cancer

Lung cancer, a highly invasive, rapidly metastasizing and prevalent cancer, is the top killer cancer in both men and women in the United States of America (USA). During 2014, an estimated 224,210 new cases and 159,260 deaths for lung cancer were predicted in the USA [1]. Lung cancer can be divided into two major histopathological groups: non-small-cell lung cancer (NSCLC) and small-cell lung cancer (SCLC). About 80% of lung cancers are NSCLC, and they are subdivided into adenocarcinomas, squamous cell, bronchoalveolar, and large-cell carcinomas [2]. Squamous cell carcinomas and adenocarcinomas are the most prominent. The remaining 20% of lung cancers show properties of neuroendocrine cells. It causes more deaths per year than the next four leading causes of cancer (colon/

rectal, breast, pancreas, and prostate) death combined in the United States. Its incidence and mortality patterns are consistently associated with 20 or more years of smoking history. The individual susceptibility to tobacco-induced lung cancer may be dependent on competitive gene-enzyme interactions that affect activation or detoxification of procarcinogens and levels of DNA adduct formation, as well as determined by the integrity of endogenous mechanisms for repairing lesions in DNA. Lung cancer is highly heterogeneous that can arise in many different sites in the bronchial tree, therefore presenting variable symptoms and signs depending on its anatomic location. 70% of patients diagnosed with lung cancer present with advanced stage disease (stage III or IV). In the Table 1 there are the most common types of lung cancer with the relative incidence and the anatomic location. Disseminate into sub mucosal lymphatic vessels and regional lymph nodes almost without a bronchial invasion.

Table 1: The most common types of lung cancer with the relative incidence and the anatomic location.

Lung Cancer Type	% of All Lung	Anatomic Location
Squamous cell lung cancers (SQCLC)	25–30%	Arise in main bronchi and advance to the carina
Adenocarcinomas (AdenoCA)	40%	Arise in peripheral bronchi
Large cell anaplastic Carcinomas (LCAC)	10%	Tumors lack the classic glandular or squamous morphology
Small cell lung cancers (SCLC)	10–15%	Derive from the hormonal cells of the lung
Cells		Disseminate into sub mucosal lymphatic vessels and regional lymph nodes almost without a bronchial invasion.

The transformation from a normal to malignant lung cancer phenotype is thought to arise in a multistep fashion, through a series of genetic and epigenetic alterations, ultimately evolving into invasive cancer. The primary cancer has a continuous accumulation of genetic and epigenetic abnormalities, acquired during clonal expansion, influences the processes of invasion, metastasis, and resistance to cancer therapy. The identification and characterization of these molecular changes are of critical importance for improving disease prevention, early detection, and treatment. The knowledge of both a patient's tumor characteristics and genetics will significantly advance the personalized prognosis and ideal treatment selection for each patient.

Several targetable genetic alterations have been identified in lung cancer [4] (Table 2), including:

- Activating mutations in a number of proto-oncogenes such as KRAS, EGFR, BRAF, PI3K, MEK and HER2. Also EGFR (epidermal growth factor receptor) plays a critical role in regulating normal cell proliferation, apoptosis, and other cellular functions. Approximately 10% of Non Small Cell Lung Cancer (NSCLC) patients in the US and 35% in East Asia have tumor associated EGFR mutations [5-7].
- Structural rearrangements in ALK, ROS1 and possibly RET.

- Amplification of proto-oncogenes such as MET in adenocarcinomas, FGFR1 and DDR2 in squamous cell lung carcinomas.
- Oncogenic gene overexpression by microRNAs (miRNAs).
- Inactivation of Tumor Suppressor Genes (TSG), including TP53, RB1, CDKN2A, FHIT, RASSF1A, and PTEN
- Enhanced telomerase activity, which contributes to cellular immortality by maintaining telomere length through de novo synthesis of telomeres and elongation of existing telomeres (100% of SCLCs and 80% to 85% of NSCLCs). The hTERT gene is amplified in 57% of NSCLCs [3].

Remarkably, scores of the aforementioned aberrations correlate with patient's smoking history as well as with racial and gender differences, which suggest a possible role of the host's genetic makeup as key determinants in lung carcinogenesis [8].

Tumor microenvironment

The tumor microenvironment. The complex interactions of its various cell types and their released signaling molecules are an emerging hallmark of cancer [9]. It consists of stromal cells, cancer-associated fibroblasts, stem cells

and a comprehensive set of immune cells recruited into tumors. The tumor microenvironment is altered to suppress host immune responses, foster tumor growth, and help cancer cells evade immune surveillance [10]. The tumor-associated immune cells include tumor-associated macrophages (TAM), dendritic cell (DC) subsets, cytotoxic and regulatory T-cells (CTLs and Tregs), natural killer (NK) cells, and myeloid-derived suppressor cells (MDSCs). The amounts of different immune cell subsets in the tumor microenvironment can vary considerably among patients and may be used as a predictor of treatment outcome and survival in certain cancers [11]. The altered tumor microenvironment is established by the cancer cells through the loss of MHC class I molecules, the loss of antigen variants, and the active secretion of several

growth factors, such as vascular endothelial growth factor (VEGF) and granulocyte-macrophage colony-stimulating factor (GM-CSF) [12]. The immune cells present in the tumor microenvironment are functionally impaired, and the newly infiltrating immune cells become alternatively activated, resulting in a perturbed phenotype [12]. Chronic inflammation can also play a significant role in the tumor environment through the release of reactive oxygen and nitrogen species, as well as TNF- α . Consequently, chronic inflammation can facilitate tumor growth via activation of NF- κ B and the subsequent suppression of adaptive immune responses [11]. NSCLC tumors often show hypoxic areas, which leads to the release of pro-angiogenic factors such as VEGF, thereby increasing tumor angiogenesis [13,14].

Table 2: Genetic alterations have been identified in lung cancer (Lemjabbar-Alaoui et al. 2015).

AKT1. AKT2. AKT3	AdenoCA (Rare). SQCLC (20%. AKT3: 16%)	PI3K
ALK	AdenoCA (3–13%)	RTK
BRAF	AdenoCA (6%). SQCLC (4%)	RAF
CCNE1	AdenoCA (12%)	RB1/CDK
DDR2	SQCLC (3–8%)	RTK
EGFR	AdenoCA (40–50%). SQCLC (7%)	RTK
ERBB2	AdenoCA (7–14%)	RTK
ERBB3	SQCLC (2%)	RTK
FGFR1	AdenoCA (1–3%). SQCLC (22%). SCLC (6%)	RTK
HRAS	SQCLC (3%)	RAS
IGF1R	SCLC (95%)	RTK
KRAS	AdenoCA (30%). SQCLC (5%)	RAS
MDM2	AdenoCA (20%)	TP53
MET	AdenoCA (25%)	RTK
MLL	SCLC (10%)	Epigenetic regulation
MYC. MYCN. MYCL	AdenoCA (31%). SQCLC (rare). SCLC (16%)	Transcriptional regulators
NKX2.1/TTF1	AdenoCA (20%)	Developmental pathways
NRAS	AdenoCA (< 1%). SQCLC (< 1%)	RAS
NRF2	SQCLC (19%)	Oxidative stress response
PIK3CA	AdenoCA (rare). SQCLC (16%)	PI3K
RET	AdenoCA (1–2%)	RTK
ROS	AdenoCA (1.5%)	RTK
SOX2	SQCLC (21%)	Developmental pathways
TP63	SQCLC (16%)	Developmental pathways
Tumor suppressor gene	Cancer type	Pathway
PTEN	AdenoCA (rare). SQCLC (8%)	PI3K
ARID1A	AdenoCA (8%)	Epigenetic regulation
ASCL4	SQCLC (3%)	Developmental pathways
CDKNA2/p16INK4	AdenoCA (> 20%). SQCLC (72%)	RB1/CK
CEBBP	SCLC (9%)	Epigenetic regulation
CUL3	SQCLC (7%)	Oxidative stress response
EP300	SCLC (9%)	Epigenetic regulation
KEAP1	AdenoCA (11%). SQCLC (12%)	Oxidative stress response
LKB1	AdenoCA (15–30%). SQCLC (2%)	LKB1/AMPK

Molecular events associated to lung cancer

Lung cancer is the leading cause of cancer deaths worldwide, the most prevalent is with non-small cell lung cancer (NSCLC) [15,16]. Most common mutations in human NSCLC are activating mutations in K-RAS (10-30%) and loss of function point mutations in p53 (50-70%) [17].

KRAS: The KRAS gene (Ki-ras2 Kirsten rat sarcoma viral oncogene homolog) is an oncogene involved in the regulation of cell division as a result of its ability to relay external signals

to the cell nucleus. RAS proteins are small GTPases, which cycle between inactive guanosine di phosphates (GDP)-bound and active guanosine triphosphate (GTP)-bound forms. RAS proteins are central mediators downstream of growth factor receptor signaling and therefore are critical for cell proliferation, survival, and differentiation. RAS can activate several downstream effectors, including the PI3K-AKT-mTOR pathway, which is involved in cell survival, and the RAS-RAF-MEK-ERK pathway, which is involved in cell proliferation [18] (Figure 1).

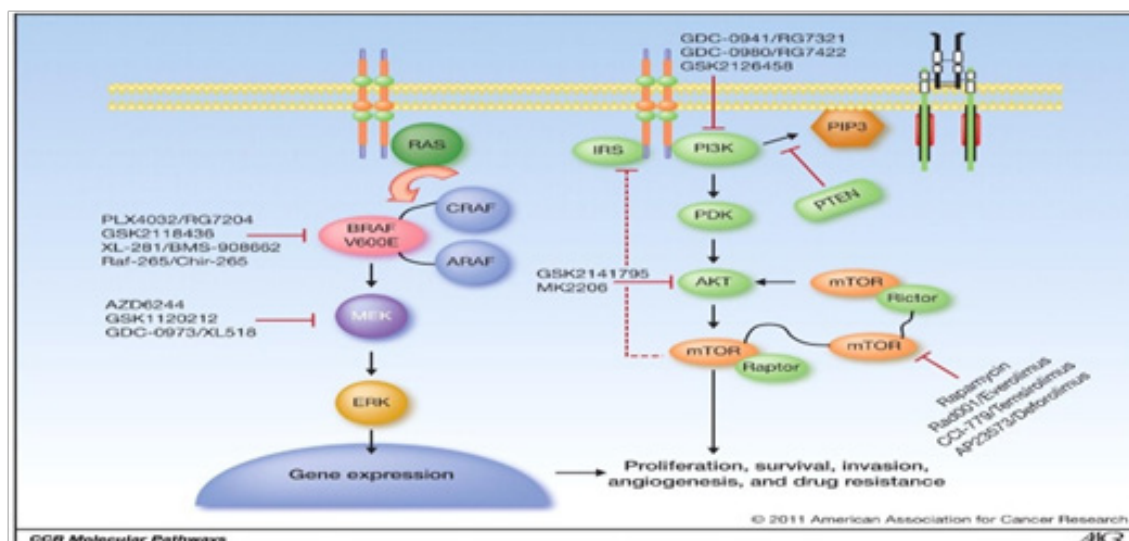


Figure 1: Schematic of the MAPK and PI3K pathways. Growth factor binding to receptor tyrosine kinase results in activation of the MAPK signaling pathway (RAS-RAF-MEK-ERK) and the PI3K pathway (PI3K-AKT-mTOR). In the absence of BRAF mutations, receptor tyrosine kinases are activated by their ligands and activate RAS and PI3K. RAS then activates the RAF/MEK/ERK signaling cascade, which eventually provides survival, proliferation, invasion, and angiogenesis advantages to melanoma tumors. BRAF mutant melanoma cells are sensitive to BRAF inhibitors, but resistance can occur via a RAF isoform switch and other compensatory pathways. Combinatorial approaches targeting more than 1 molecule within 1 pathway or several pathways simultaneously need to be carefully investigated as potential treatment options for melanomas refractory to BRAF inhibitors. Compounds targeting the MAPK and PI3K pathways, and those currently being tested in clinical trials, are indicated.

Mutations in the KRAS gene impair the ability of the KRAS protein to switch between active and inactive states, leading to cell transformation, increased resistance to chemotherapy and biological therapies targeting epidermal growth factor receptors. KRAS mutations are particularly common in colon cancer, lung cancer, and pancreatic cancer. Since when, it has been accepted that KRAS is one of front-line sensors that initiate the activation of an array of signaling molecules allowing the transmission of transducing signals from the cell surface to the nucleus, thus affecting cell differentiation, growth, chemotaxis, and apoptosis. A signal transduction cascade initiated by the activated form of KRAS is depicted in Figure 2. As a result of these effects, KRAS elicits changes in the cytoskeleton and consequently affects cell shape, adhesion and migration [19,20].

a. Regulation of KRAS Gene Expression

The transcription of KRAS is regulated, in part, by an interaction between the promoter region and the 65 kDa ESXR1 proteins and, in part, by miRNAs. ESXR1 is a human protein with an N-terminal homeodomain in the

nucleus and a C-terminal proline-rich repeat region I in the cytoplasm. The N-terminal fragment of ESXR1 binds exon-1 of the KRAS gene, thus inhibiting its mRNA expression [21]. miRNAs contain a 21-22 nucleotide long no coding sequence that is able to regulate gene expression [22]. KRAS expression is regulated both during the initiation of transcription by the binding of proteins to its promoter and during transcriptional elongation by microRNAs affecting KRAS mRNA stability. While miRNAs and the KRAS oncogene are known to be dysregulated in various cancers, little is known about the role of miRNAs in the regulation of KRAS in cancer.

b. KRAS in oncogenesis

Activating KRAS gene point mutations have been detected in many types of human tumors [23]. Such oncogenic forms of the KRAS gene are prevalent in pancreatic carcinomas (>80%), colon carcinomas (40-50%), and lung carcinomas (30-50%), but are also present in biliary tract malignancies, endometrial cancer, cervical cancer, bladder cancer, liver cancer, myeloid leukemia [24] and breast cancer.

Mutations in the KRAS gene have important effects on the process of carcinogenesis, which depend on the cells and tissues involved [25]. Analyses of human cancer cell RAS genes showed that they differed from those in normal cells in single nucleotides of codons, such as 12, 13, 59, 61, and

63; hot spot mutations in exons 1 and 2 were associated with transforming activities. These mutations are located near to the GTP binding site. Allelic mutations result in amino acid changes, namely Gly to Asp, Ala, Arg, Ser, Val, or Cys in codon 12 and Gly to Asp in codon 13 [26].

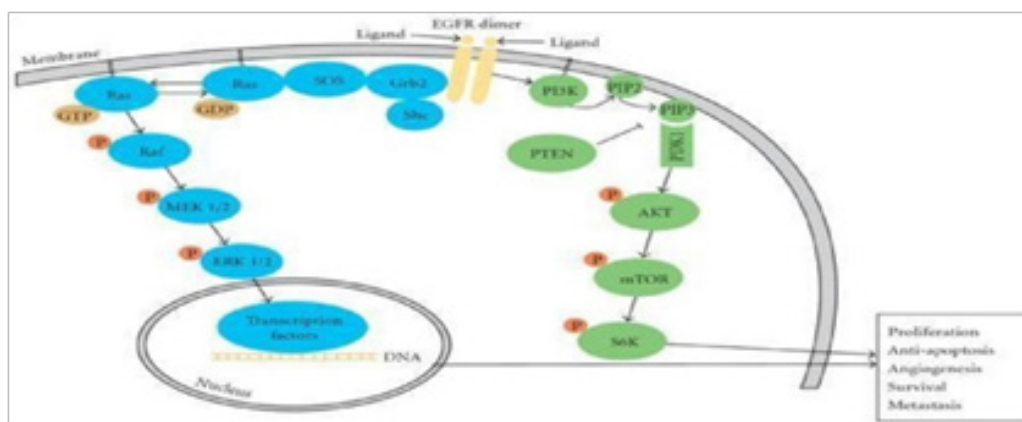


Figure 2: Signaling pathway of the KRAS protein. Following EGF binding to its receptor and activation of tyrosine kinases, the KRAS protein becomes activated by binding to GTP, transducing the activation signal to the nucleus by MAPKs and PI3K/AKT-mediated cascades. Specifically, the active state of the KRAS protein is facilitated by binding to the Grb2 protein, which interacts with the SH3 domains of the SOS protein, a member of the nucleotide exchange factor family. In the GTP state, KRAS is able to activate downstream proteins and to regulate cell transformation.

Mutation in codon 12 of the KRAS gene causes the encoded KRAS protein to “freeze” in its active state for a much longer duration than its non mutated counterpart [27]. The oncogenic forms of the RAS protein have a profound effect on the downstream effector pathways, resulting in much higher proliferation rates of cancer cells expressing such forms. Overexpression of KRAS can also be induced by the loss of p16INK4 (CDKN2A), p19INK4 (CDKN2D), or p53 [28]. However, studies by Zhang et al. [29] have shown that the wild-type KRAS allele can suppress the oncogenic function of the mutated.

c. KRAS in Non-Small Cell Lung Cancer (NSCLC)

Losses of KRAS wild type alleles in both mouse and human lung adenocarcinomas and squamous carcinomas have been found in many studies, notably in 67% to 100% of chemically induced murine lung adenocarcinoma cases harboring a mutant KRAS. Mutations in the KRAS gene in codons 12 and 13 were detected in 21% of NSCLC (non-small cell lung cancer) tumor samples examined in the TRIBUTE III trial [30]. They are rarer in never smokers and are less common in East Asian vs. US/European patients [31,32]. NSCLC patients have a tendency to accumulate activating mutations in either the EGFR or KRAS genes. However, a clinical study has shown that mutations of these two genes are, in general, mutually exclusive. EGFR mutations are more often found in patients who have no history of smoking. The role of KRAS as either a prognostic or predictive factor in NSCLC is unknown at this time. Very few prospective randomized trials have been completed using KRAS as a biomarker to stratify therapeutic options in the metastatic setting.

P53

The p53 pathway responds to stresses that can disrupt

the fidelity of DNA replication and cell division. A stress signal is transmitted to the p53 protein by post-translational modifications. This results in the activation of the p53 protein as a transcription factor that regulates several genes with a broad range of functions, including DNA repair, metabolism, cell cycle arrest, apoptosis and senescence. The p53 pathway is composed of a network of genes and their products that are targeted to respond to a variety of intrinsic and extrinsic stress signals that impact upon cellular homeostatic mechanisms that monitor DNA replication, chromosome segregation and cell division [33]. The p53 protein is activated in a specific manner by post-translational modifications, and this leads to either cell cycle arrest, a program that induces cell senescence or cellular apoptosis [34]. In this way, a variety of intrinsic or extrinsic stresses that would result in a loss of fidelity in DNA replication, genome stability, cell cycle progression or faithful chromosome segregation can be accommodated or, alternatively, the clone of cells with these defects eliminated from the body. P53-regulated and p53-secreted proteins may alter the extracellular matrix and influence angiogenic signals in a localized region of a tissue. After DNA damage in a cell, the p53 pathway produces a set of proteins that can aid directly in DNA repair processes. Finally, the activation of the p53 protein and its network of genes sets in motion an elaborate process of auto regulatory-positive or auto regulatory-negative feedback loops, which connect the p53 pathway to other signal transduction pathways in the cell.

Nature of the stress signals that activate p53 and its pathway

Stresses, both intrinsic and extrinsic to the cell, can act upon the p53 pathway. Among the signals that activate the p53 protein is damage to the integrity of the DNA template. Gamma or UV irradiation, alkylation of bases, deprivation of

DNA or reaction with oxidative free radicals all alter the DNA in different ways, and for each damaging agent, a different detection and repair mechanism is employed by the cell [35,36]. In each case the proteins that detect and repair the DNA lesion contain enzyme activities that communicate

to the p53 protein that the DNA is damaged. This is accomplished by post-translational modifications resulting in phosphorylation, acetylation, methylation, ubiquitination or sumolation of the p53 protein (Figure 3) [37].

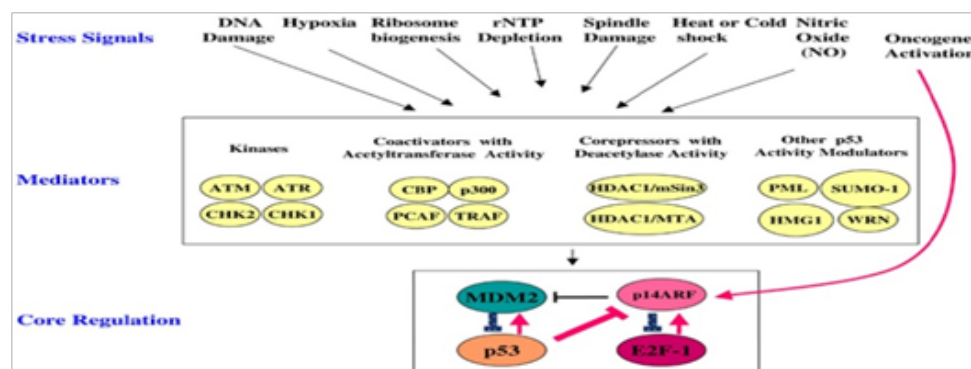


Figure 3: Diversity of cancer-related signals that activate p53 contributes to the central role the p53 protein as a tumor suppressor. See text for details.

A mutation or alteration in a selected protein that signals inappropriately for entry into the cell cycle is detected by the p53 checkpoint and this cell is usually killed. This is an excellent example of the tumor suppressor phenotype of the p53 protein [38]. The activation of the p53 protein in response to stresses is mediated and regulated by protein kinases, histone acetyl-transferase, methylases, and ubiquitin and sumo ligase. Once the p53 protein is activated, it initiates a transcriptional program that reflects the nature of the stress signal, the protein modifications and proteins associated with the p53 protein. The genes in this p53 network initiate one of three programs that result in cell cycle arrest (G-1 or G-2 blocks are observed), cellular senescence or apoptosis (Figure 4). A major player in the p53-mediated G-1 arrest is the p21 gene product that inhibits cyclic E-cdk2. This cyclic-dependent kinase act upon the Rb protein to derepression the E2F1 activity that promotes the transcription of genes involved in preparing a cell to progress from G-1 to S phase in the cell cycle. The p53-induced G-2 arrest is mediated in part by the synthesis of 14-3-3 sigma, a protein that binds to CDC25C and keeps it in the cell cytoplasm. CDC25C is a phosphatase that acts upon cyclic B-CDC2, a kinase that is essential for the G-2- to M-phase transition. Keeping CDC25C in the cytoplasm prevents it from activating cyclic B-CDC2 in the nucleus and these cells are blocked in the G-2 phase of the cell cycle (Figure 4) [39].

P53 is inactivated by mutations in over 50% of all cancers. Such mutations can disrupt its direct binding to DNA or lead to structural perturbations that prevent the correct folding or oligomerization of the tumor suppressor. At other times, loss of p53 function is due to overexpression of p53-regulatory proteins that suppress p53 activity, such as MDM2 and MDMX. In mouse models, the absence of p53 leads to the development of spontaneous tumors, notably in the thymus. Numerous strategies have been devised to correct a dysfunctional p53-regulatory pathway. Small-

molecule inhibitors of the p53-MDM2 interaction, p53 gene therapies and drugs that act as chaperones by binding to mutant p53 and restoring its function are some of the approaches currently in clinical trials. The mutations that inactivate p53 function in cancer cells almost all appear to localize to the DNA-binding domain of the p53 protein and produce a protein that fails to transcribe p53- responsive genes. Thus, the cancer cell appears to select for the loss of transcription factor activity. When fragments of the p53 protein inactive for transcription are overexpressed in HeLa cells in culture, they can induce an apoptosis [40]. Whether this is a consequence of an overexpression activity and has no physiological significance or this means that p53 even without its transcription factor activity can act to kill cells remains a debatable issue in the literature. Similarly, p53 mutant proteins have been shown by many research groups to have a ‘gain-of-function’ phenotype [41,42], resulting in enhanced tumorigenic potential, enhanced drug resistance and even allele- specific phenotypes.

Feedback loops in his p53 pathway

Feedback loops of the type described here provide a means to connect the p53 pathway with other signal transduction pathways and coordinate the cellular signals for growth and division. Redundancies in a system can sometimes prevent errors and a backup system reduces the phenotype of mutations. Many of these pathways have been elucidated by experiments carried out with cancer cells in culture that have mutations that alter these pathways. Even normal cells in culture or knockout mice may not reflect all the conditions that occur in normal cells and organs in vivo. It is particularly difficult to prove that a specific protein kinase or phosphatase acts upon a specific substrate in vivo and has an outcome that can be measured quantitatively. However, these constructs are useful in formulating hypotheses and testing ideas that will surely lead to novel insights into the nature of cancers and the design of drugs and agents that selectively kill cancer cells.

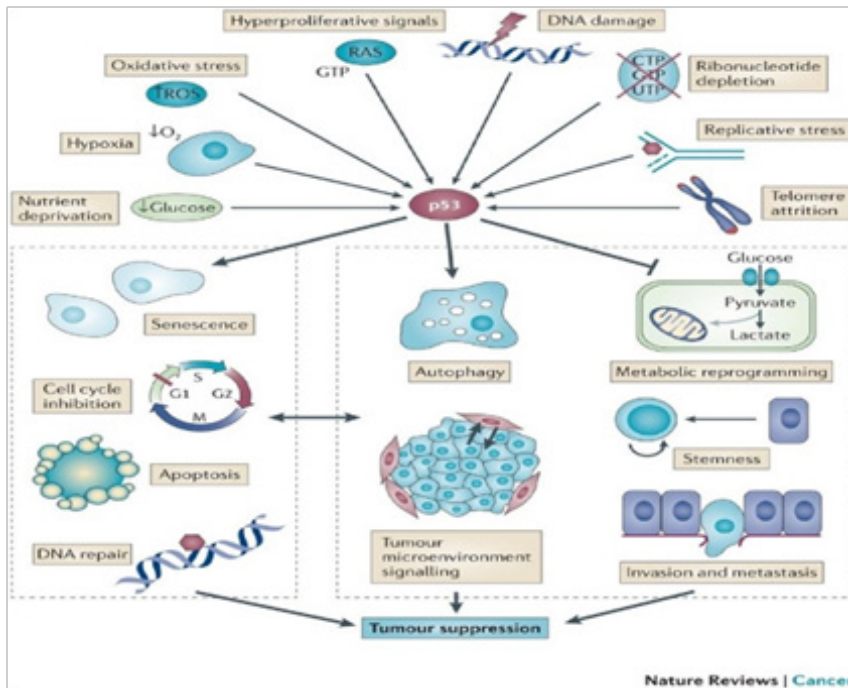


Figure 4: A host of different stresses can activate p53 in the context of tumour initiation or progression, including nutrient deprivation, hypoxia, oxidative stress, hyperproliferative signals (which could also promote chronic DNA damage or oxidative stress), DNA damage (which might most typically be chronic DNA damage triggered by replicative stress, telomere attrition, or oxidative stress), and ribonucleotide depletion. p53 activation by these signals, or potentially even 'basal' p53 action in some contexts, can consequently promote diverse responses that lead to tumour suppression. This view expands the set of stress signals that can activate p53 to promote responses of cell cycle arrest, senescence, apoptosis and DNA repair, which could potentially occur through pathways that are distinct from those used upon acute DNA damage.

Pin1

Protein phosphorylation orchestrates the activation of signaling cascades in response to extra- and intracellular stimuli to control cell growth, proliferation and survival. These signaling events often include conformational changes in protein kinases and their substrates. Such conformational changes are involved in specific signaling mechanisms that regulate a spectrum of protein activities in physiological processes and diseases such as cancer [43,44].

Proline-directed protein phosphorylation is a common and central signaling mechanism that has crucial roles in diverse cellular processes and controls cell proliferation and

transformation, and its dysregulation contributes too many human cancers [45]. Enzymes that are responsible for such phosphorylation belong to a large superfamily of proline-directed protein kinases, which include cyclic-dependent protein kinases (CDKs), mitogen-activated protein kinases (MAPKs), including extracellular signal- regulated kinases (ERKs), stress-activated protein kinases/c-Jun N-terminal kinases (SAPKs/JNKs), and p38 kinases, glycogen synthase kinase 3 (GSK3) and Polo-like kinases (PLKs) (Lu & Zhou 2007). Proline exists in one of two distinct conformers, *cis* and *trans*. Peptide polyol *cis/trans*isomerases (PPIase) catalyze the *cis-trans* isomerization of peptide polyol bonds, and this *cis-trans* rotation of the peptide bond affects the spatial arrangement of the backbone segments in the proteins (Figure 5).

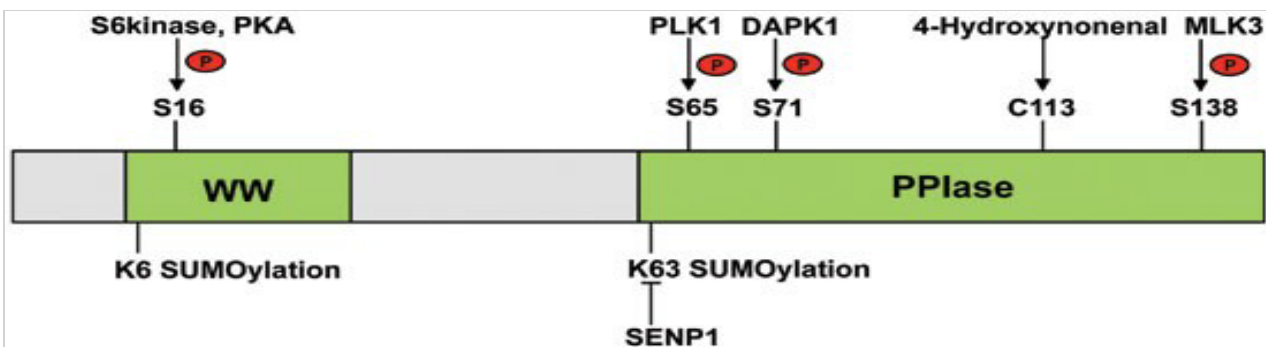


Figure 5: Schematic of the structure of Pin1 showing the regulatory posttranslational modification sites.

The three phylogenetically conserved PPIase families are cyclophilins, FK506-binding proteins and pavilions [46]. Protein interacting with never in mitosis A1 (Pin1), which is a member of the parvula subfamily of PPIase and was originally identified in 1996 [47], specifically recognizes phosphorylated serine (S) or threonine (T) residues in pSer/Thr-Pro peptide sequences [47-49].

Pin1 has a modular domain architecture consisting of an N-terminal WW domain, a flexible linker and a C-terminal parvulin-type catalytic PPIase domain (Figure 6). The WW domain is responsible for Pin1's binding to pSer/Thr-Pro motifs in substrate proteins [46], and thus catalyzes the interconversion between both conformations [50].

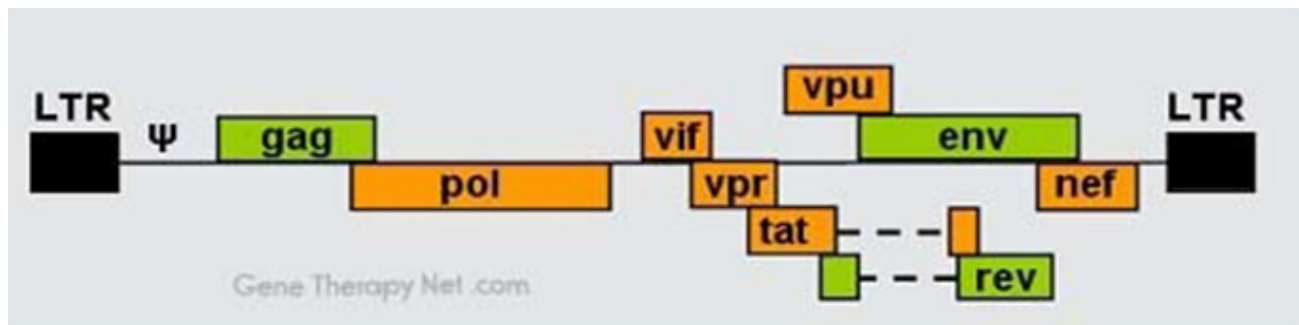


Figure 6: Genome organization of lentiviruses. Viral proteins involved in early stages of replication include Reverse Transcriptase and Integrase. Reverse Transcriptase (RT) is the virally encoded RNA-dependent DNA polymerase. The enzyme uses the viral RNA genome as a template for the synthesis of a complementary DNA copy. RT also has RNaseH activity for destruction of the RNA-template. Integrase (IN) binds both the viral cDNA generated by RT and the host DNA. Processing of the LTR by IN is performed prior to insertion of the viral genome into the host DNA. Although transmission is generally via infectious particles, lentiviruses are capable of infecting neighboring cells in direct contact with the host cells, without having to form extracellular particles [82].

Pin1 can also regulate the stability of substrate proteins by increasing or decreasing their ubiquitylation, working with different E3 ubiquitin ligase to regulate degradation of proteins. Pin1 mediates conformational changes in its substrate proteins. However, some of Pin1's functions could be mediated simply by binding of its WW domain to pS/T-P motifs (i.e., a scaffolding activity) without involving its catalytic activities. Pin1 is regulated by extra- and intracellular stimuli, and governs the structures and functions of a broad range of signaling molecules, thus playing a pivotal role in tumor cell growth, survival, migration, invasion and metastasis. Mouse models have been used to investigate the critical roles of Pin1 in regulating tumor development. Transgenic overexpression of Pin1 in mouse mammary glands induces centrosome duplication, chromosome missegregation and Aneuploidy, and results in mammary hyperplasia and malignant mammary tumors [51]. In addition, Pin1 ablation in mice is highly effective in preventing oncogenic Her2 or Ha-Ras from inducing cyclic D1 expression and mouse mammary gland carcinoma [52]. Furthermore, Pin1 ablation in p53-knockout mice inhibits p53 deficiency-induced formation of lymphomas [53]. These findings support an instrumental role of Pin1 in promoting tumor development.

a. Pin1 expression in human cancer

Pin1 overexpression is prevalent in human cancers and its expression in several types of human cancer is frequently found to be higher than that in their normal counterparts [54]. Moreover, Pin1 expression has been linked to cancer prognosis. Pin1 overexpression positively correlates with a higher probability of and a shorter time to tumor recurrence, poor survival and lymph node metastasis in non-small cell lung cancer patients [55,56]. In addition, Pin1 expression has been found to correlate with other tumor markers in humans, which supports an important theory about the role

for Pin1 in tumorigenesis and tumor progression. Pin1 can be regulated both transcriptionally and posttranslational. However, whether PIN1 is amplified in cancer has not been intensively studied.

Death-associated protein kinase 1 (DAPK1) phosphorylates Pin1 at S71 in the PPIase catalytic active site to inactivate Pin1's catalytic activity and inhibit Pin1's nuclear localization and cellular function [57]. In contrast, mixed-lineage kinase 3 (MLK3), a MAPK kinase kinase (MAP3K) family member, phosphorylates Pin1 at S138 in the PPIase domain to increase its catalytic activity and nuclear translocation [58]. In addition, PLK1-dependent phosphorylation of Pin1 at S65 in the PPIase domain, which prevents the ubiquitylation and proteasome-dependent degradation of Pin1 without affecting its isomerase activity, stabilizes Pin1 [59]. The binding of Pin1 to its substrates can also be regulated by Pin1 phosphorylation.

Oxidative stress induces lipid electrophiles to target Pin1 for modification, which disrupts Pin1 activity by forming an adduct with Pin1 at C113, a residue in the active site that is essential for catalytic activity. SUMOylation is another regulatory modification for Pin1. SUMOylation of Pin1 on K6 in the WW domain and on K63 in the PPIase domain inhibits Pin1's activity and oncogenic function. SUMOylated Pin1 can be deSUMOylated by SUMO protease 1 (SEN1), which increases Pin1 protein stability. Overexpression of SEN1 or disruption of Pin1 SUMOylation by mutations promotes Pin1's ability to induce centrosome amplification and cell transformation [60]. Protein phosphorylation regulated by protein kinases and phosphatases is involved in every important cellular activity in eukaryotic cells [61]. Pin1 regulates the functions of protein kinases and phosphatases at the plasma membrane, cytosol and nucleus.

b. Pin1 modulates protein kinase and phosphatase actions in cell cycle regulation

Cell cycle progression requires orchestrated changes in the activity or expression levels of a variety of key signaling proteins. G protein-coupled receptor kinase 2 (GRK2), which plays a central role in G protein-coupled receptor regulation, is phosphorylated by the cyclic-dependent kinase 2 (CDK2) at S670 near the C-terminus. This phosphorylation triggers GRK2's binding to Pin1 and its subsequent degradation during the G2/M transition. Prevention of GRK2 phosphorylation at S670 by mutation to Ala impedes normal GRK2 downregulation and markedly delays cell cycle progression in a receptor-independent fashion. Doxorubicin-induced activation of the G2/M checkpoint stabilizes GRK2 levels, which inversely correlate with the p53 response and the induction of apoptosis [62.].

The cyclic-dependent kinase CDC2/cyclic B complex regulates mitosis entry and progression. CDC2 is negatively regulated by phosphorylations at its T14 and Y15 residues, which are mediated by the Myt1 and Wee1 kinases, respectively. Pin1 interacts with Myt1 and potentially modulates mitosis entry [63]. The interaction between Pin1 and phosphorylated CDC25 promotes a conformational change in CDC25 and increases its ability to activate and maintain CDC2/cyclic B activity, suggesting that Pin1 modulates cell cycle control through its interaction with CDC25 and its regulation of CDC25-dependent CDC2/cyclic B activity [64,65].

c. Pin1 regulates transcription factors and transcription regulators

It including cyclic D1, cyclic E and c-Myc in central pathways important for tumor development

Cyclic D1, which is important for cell cycle progression and cell proliferation, is a direct substrate of Pin1. Pin1 binds to cyclic D1 phosphorylated at Thr286-Pro by GSK3 β and increases cyclic D1 levels in the nucleus and stabilizes cyclic D1. Pin1-deficient mice and cyclic D1-deficient mice share characteristics that include retinal hypoplasia and impaired mammary gland development. In pregnant Pin1-deficient mice, cyclic D1 levels are significantly reduced in many tissues, including the retina and breast epithelium, and these mice fail to undergo the massive proliferative changes in breast epithelium associated with pregnancy [66,67].

Besides regulating cyclic D1 expression, Pin1 also regulates the stability of cyclic E. Pin1's binding to the cyclic E-CDK2 complex depends on CDK2-mediated phosphorylation of cyclic E at S384 [68], which promotes cyclic E degradation mediated by the sequential functions of SCF-Fbw7 α and SCF-Fbw7 γ . Oncogenic Ras activity both inhibits cyclic E-Fbw7 binding and cyclic E ubiquitylation, and potentiates cyclic E-induced genetic instability, which may serve as a mechanism through which Ras mutations promote tumorigenesis [69].

d. Pin1 regulates nuclear receptors

Estrogen receptor- α (ER α), a nuclear receptor expressed in breast epithelial cells, functions as a hormone-regulated transcription factor. Activation of the PI3K pathway promotes the nuclear translocation of CDK2 and phosphorylation of CDK2 at T160 in activation site [103]70. Activated CDK2 in turn phosphorylates ER α at S294 and mediates Pin1-ER α interaction, which increases ERK-dependent ER phosphorylation at S118 and S167 in the transcriptional activation function domain and promotes ER α dimidiation and activity [71,72]. Pin1 has also been shown to bind to ER α pS118 directly and cause the *cis-trans* isomerization of the pS118-P119 bond of ER α . This isomerization stabilizes ER α protein by blocking ER α interaction with the E3 ligase, E6AP, and thus inhibiting the E6AP-mediated ubiquitylation and degradation of ER α . In addition, Pin1 and ER α levels are positively correlated in human breast carcinoma specimens [71,73,74]. Pin1 also promotes the activation of nuclear receptor-regulated transcription by interacting selectively with phosphorylated steroid receptor coactivator 3 (SRC-3/AIB1/pCIP) and modulating interactions between SRC-3 and cyclic adenosine monophosphate response element binding protein (CREB)-binding protein (CBP)/p300 coactivators [75].

e. Pin1 regulates transcription factors and co-regulators involved in tumor suppression and growth inhibition

In addition to transcription regulators that promote tumorigenesis, Pin1 also regulates a large number of tumor suppressors and growth inhibitors, including Smad transcription factors, the co-repressor silencing mediator for retinoic acid and thyroid hormone receptor (SMRT), forehead box O (FOXO), promyelocytic leukemia protein (PML), runt-related transcription factor 3 (RUNX3), the retinoblastoma protein (pRb), p53 and p73 [76,77]. Disruption of transforming growth factor- β (TGF- β) signaling, which is crucial in numerous cellular processes including proliferation, differentiation, migration and apoptosis often occurs in cancer. pRb represses gene expression, and hyperphosphorylation of pRb releases its inhibition of E2F transcription factors. Pin1 directly interacts with CDK-phosphorylated S608/612 in the spacer domain of pRb, which enables the interaction between CDK/cyclic complexes and pRb in middle and late G1 phase and promotes pRb S780 phosphorylation. pRb deficiency abrogates the Pin1 deficiency-induced inhibitory effect on cell proliferation, further supporting the hypothesis that pRb is a substrate of Pin1 [71,77].

The tumor suppressor p53 is important in cell cycle arrest or apoptosis in response to a variety of stimuli. In response to DNA damage, p53 interacts with Pin1, and this interaction is dependent on p53 phosphorylations. The binding of Pin1 to p53 elicits conformational changes in p53 and stimulates its DNA-binding activity and transactivation function towards the *p21* promoter. Moreover, Pin1-deficient cells are defective in p53 activation and the timely accumulation of p53 and have impaired checkpoint control in response to DNA damage [78-80]. The physiological relationship between Pin1 and p53

was also demonstrated using *Pin1*^{-/-}*p53*^{-/-} mice, which showed that development of lymphomas in p53-deficient mice was inhibited by Pin1 ablation. In addition, Pin1 plays an important role in mutant p53- promoted transformation and metastasis. Pin1 promotes the mutant p53-dependent inhibition of the anti-metastasis factor p63 and promotes the induction of a mutant p53 transcriptional program to increase tumor aggressiveness. Pin1 also cooperates with mutant p53 in Ras-dependent transformation to enhance tumorigenesis. Furthermore, in breast cancer patients, the combination of Pin1 overexpression and p53 mutation is an independent prognostic factor for poor clinical outcome [81]. These results suggest that Pin1 impacts p53 function at multiple levels [53].

f. Pin1 expression contributes to lung cancer

Pin1 protein was shown to be overexpressed in NSCLC tumor samples, and correlated with lymph node positive disease and tumor stage. High expression of MDM2 also correlated with lymph node positive disease and with poorly differentiated tumors. High expression levels of Pin1 correlated with high levels of p53 or MDM2 protein, but did not show a correlation with cyclic D1. However, high levels of MDM2 correlated with cyclic D1 overexpression. Pin1 mRNA was expressed significantly more often in the tumors of smokers than of non-smokers. The relationship between the expression of protein and mRNA of Pin1 has obviously showed that protein expression isn't significantly associated with mRNA expression. Pin1 is overexpressed in many different cancers, including NSCLC, and may possibly be

used as a tumor marker or as a target for cancer therapy. Current therapies for NSCLC patients are inefficient due to the lack of diagnostic and therapeutic markers. The phospho-Ser/Thr-Pro specific prolyl-isomerase Pin1 is overexpressed in many different cancers, including NSCLC, and may possibly be used as a target for cancer therapy.

Lentivirals vectors

Lentivirus is a genus of the Retroviridae family, characterized by a long incubation period. Lentiviruses can deliver genetic information into the DNA of the host cell, so they are one of the most efficient methods of a gene delivery vector. Lentivirus is a research tool used to introduce a gene product or edit the genome of in vitro systems or animal models through gene editing techniques like cre-lox or Crispr/Cas, but it has a wide use for therapeutic applications. It is important where stable long-term integration or deletion of the gene is required, in addition, lentiviral vectors can infect a wide variety of cell types and have a relatively low toxicity profile when compared to the other virus vectors for this reason they have been extensively represented in clinical trials. Examples of lentivirus are HIV, SIV, and FIV [82]. Infectious lentiviruses have three main genes coding for the viral proteins in the order: 5'- gag-pol-env-3' (Figure 7). There are accessory genes (e.g., for HIV-1: *vif*, *vpr*, *vpu*, *tat*, *rev*, *nef*), they are involved in regulation of synthesis and processing viral RNA and other replicative functions. The LTR is about 600nt long, of which the U3 region is 450, the R sequence 100 and the U5 region some 70nt long.

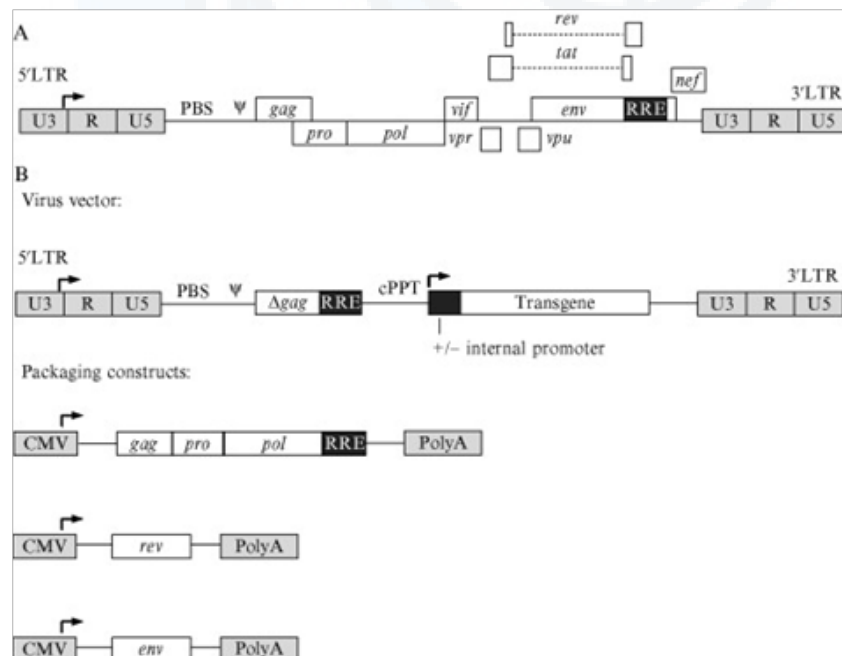


Figure 7: Schematic representation of the proviral genomic structure of lentiviruses and derivative vectors. (A) Proviral wild-type DNA of a typical lentivirus: The gag, pro, pol, env, and associated accessory genes, coding regions are indicated together with the U3, R, and U5 regions of the 3'- and 5'-long terminal repeats (LTRs). The primer binding site (PBS), packaging signal (Ψ), central polypurine tract (cPPT), and rev response element (RRE) regulatory regions in cis are also shown. (B) General structure of lentiviral-derived vectors showing the mutated gag sequence (Δgag), cPPT, and RRE upstream of the transgene. Arrows indicate the U3 and internal promoter regions. Packaging constructs containing gag, pro, and pol sequences together with the RRE, the rev sequence, and the env sequence with polyA tracts under the control of the cytomegalovirus (CMV) promoter are shown below [87].

Large-scale collaborative efforts are underway to use lentiviruses to block the expression of a specific gene using RNA interference technology in high-throughput formats. The expression of short-hairpin RNA (shRNA) reduces the expression of a specific gene, thus allowing researchers to examine the necessity and effects of a given gene in a model system. Another common application is to use a lentivirus to introduce a new gene into human or animal cells. Retroviruses are useful tools for the efficient delivery of genes to mammalian cells, owing to their ability to stably integrate into the host cell genome. Over the past few decades, retroviral vectors have been used in gene therapy clinical trials for the treatment of a number of inherited diseases and cancers.

Vectors based on lentiviruses like HIV-1 are able to transduce both dividing and non dividing cells [83]. This ability is due to the fact that the PIC of lentiviruses is able to enter the nucleus without disrupting the nuclear membrane. Nuclear translocation is facilitated by proteins and accessory protein. For example the MA protein has also been shown to bind directly to importin- α , facilitating entry of the PIC through nuclear pores [84] or the accessory protein Vpr binds directly to the nuclear pore complex and causes transient herniations in the nuclear membranes [85]. In addition to Vpr, lentiviruses encode a number of other accessory proteins Vif, Vpu, Tat, Rev, and Nef (Figure. 2.2A). Only Tat and Rev are strictly required for virus replication. Tat activates the promoter of the HIV LTR so that viral RNA is produced more efficiently, and Rev interacts with a region of RNA known as the Rev Response element (RRE) to promote the transport of viral RNA from the nucleus into the cytoplasm [86]. The larger genomic size of HIV-1 and other lentiviruses means that large or multiple transgenes can be incorporated into vectors developed from these viruses.

In lentiviral vectors, the cis-acting elements are similar to that of retroviruses, but the additional cPPT and RRE regions are also present upstream of the transgene. Additional elements increases the risk of homologous recombination events, thus the gag-pro-pol, rev, tat, and env genes are all provided in trans on separate expression constructs to reduce the risk of such events [88]. Third-generation lentivirus vectors currently in use have a self-inactivating (SIN) design which negates the use of Tat. The generation of helper cell lines for lentivirus vectors has proved difficult because some of the lentivirus proteins are toxic to cells leading to low vector titers. Lentivirus vectors are usually produced by transient transfection methods, and pseudo typing lentivirus vectors with the surface glycoprotein from vesicular stomatitis virus G protein (VSV-G) have helped to increase stability and titer, as well as broaden the tropism.

Retrovirus and Lentivirus Vector Design

Various factors must be considered for virus vector design, like the choice of transgene. Transgenes selected for therapeutic applications normally have very defined functions, and mutations lead to loss or gain of very specific phenotypic characteristics. Genes involved in cell cycle regulation, cellular proliferation, and apoptosis pose

particular problems for therapeutic applications in humans as they are often involved in multiple signaling pathways. Non physiological expression may lead to deleterious effects such as tissue damage or cancer, so-called phenotoxicity. Other factors to consider are whether the gene is ubiquitously expressed or only expressed in specific cells and tissues, and the level of protein expression in different tissues.

The promoter, Marker genes and Enhancer regions

If a ubiquitously expressed is encoded by the gene of interest, internal heterogenous promoters can be used to drive transgene expression. However, the protein is not ubiquitously expressed but found in specific cell types, for example, cells of the hematopoietic system, then it may be preferable to use a promoter that is cell type specific, such as that described for the Wiskott-Aldrich syndrome gene [89]. The construction of artificial promoters allows acting with specificity. Virus vectors and packaging constructs often contain antibiotic resistance genes such as ampicillin or kanamycin. These antibiotic resistance genes permit the transformation of electrically or chemically competent *Escherichia coli* for the propagation of constructs. Selectable markers for other types of antibiotic resistance such as G418 are used for selection of mammalian cells transfected with packaging constructs to generate stably expressing packaging cell lines.

A vector has to contain a marker gene to monitor the expression before testing the transgene of choice. This enables troubleshooting of any problems associated with the vector backbone, promoter, cis-elements, or packaging constructs prior to testing the transgene itself. One of the most common marker proteins is the enhanced green fluorescent protein (eGFP), it is easily monitored by flow cytometry or confocal microscopy. Truncated versions of cell surface proteins such as CD34 and low-affinity nerve growth factor receptor can also be used as cell surface markers. These proteins retain their extracellular and TM regions but lack intracellular domains and therefore do not affect cell function. When live imaging is required, the luciferase reporter gene is a useful marker for tracking gene expression in vivo in real time [87].

Safety considerations and Vector Production

Gamma retroviral vectors have a propensity to integrate near regulatory regions (including transcription start sites) of active genes (De et al., 2005 and Wu et al., 2003). The activity of promoter/enhancer elements within the vector LTRs or aberrant splicing events can lead to the activation of genes flanking the integration site (Hacein-Bey-Abina et al., 2008 & Howe et al., 2008). This is commonly referred to as insertional mutagenesis. If the genes near the integration sites are proto-oncogenes, this may lead to increased proliferation of clonal populations of cells. This has been observed in several patients with SCID-X1 and Wiskott-Aldrich syndrome treated with gamma retroviral vectors who developed T cell leukemias, and in the patients with CGD who developed dominant myeloid clones. Analysis

of clonal populations of lymphoid cells from four of the SCID-X1 patients and one WAS patient revealed that the mutagenic retrovirus integration site was located near the promoter of the LMO2 gene, a proto-oncogene associated with acute T cell leukemias (Hacein-Bey- Abina et al., 2008 and Howe et al., 2008).

A number of packaging cell lines are commercially available for the generation of gamma retrovirus vectors and the choice of system depends on the envelope protein required (Miller, 1997). Phoenix packaging cells lines, based on HEK 293T cells, express the MLV gag- pro-pol and env proteins and offer the advantage that these cells have high protein expression levels of these viral coding sequences, allowing for higher virus vector titers to be achieved. Two variations are available that allow pseudo typing with either amphotropic (Phoenix-Ampho) or ectotropic (Phoenix-Eco) envelope proteins. There is also a Phoenix-gp cell line which expresses only gag-pro-pol enabling pseudotyping of the retroviral vector with other envelop proteins such as GALV or VSV-G.

Lung Cancer Mouse Conditional Model

Lung cancer can be divided into two major histopathological groups: non-small-cell lung cancer (NSCLC) (Van Zandwijk et al. 1995) and small-cell lung cancer (SCLC) [16]. They show major differences in histopathologic characteristics that can be explained by the distinct patterns of genetic lesions found in both tumor classes (Zochbauer-Muller et al. 2002). Responsiveness to treatment with chemotherapy and/or radiation also differs significantly between NSCLC and SCLC and has a dramatic effect on clinical treatment outcome. Mouse models for lung cancer can thus serve as a valuable tool not only for understanding the basic lung tumor biology but also for the development and validation of new tumor intervention strategies as well as for the identification of markers for early diagnosis.

Similarities in genotype-phenotype correlations, morphology, histopathology along with tumor cell characteristics between lung tumor in mice and man [2,90] make mouse models a valuable tool for understanding fundamental biologic mechanisms underlying the ontogeny of different histopathological groups of lung tumors (non-small cell lung cancer (NSCLC) and small cell lung cancer (SCLC) [2]. In addition, mouse models for lung cancer serve as important means to identify markers for early diagnosis and verify novel strategies of therapeutic intervention.

Somatic mouse models are based on the ability to activate or inactivate specific alleles, and in a tissue-specific cell type. The resulting conditional somatic mouse models can be used as versatile powerful tools in basic cancer research and preclinical translational studies alike. These models permit us to investigate initiation (cell of origin) and progression of lung cancer, along with response and resistance to drug therapy. Cre/lox or FLP/frt recombinase-mediated methods are now well-used techniques to develop tissue-restricted lung cancer in mice with tumor-suppressor gene and/or oncogene (in) activation. Intranasal

or intratracheal administration of engineered adenovirus-Cre or lentivirus-Cre has been optimized for introducing Cre recombinase activity into pulmonary tissues.

The advantage and disadvantage of commonly used mice models for lung cancer:

a. Conventional transgenic

Advantages: quick, technically easy and applicability to a wide variety of species.

Disadvantage: potential embryonic or prenatal lethality of some transgenes, strong cancer predisposition bias, stochastic transgene expression.

b. Conditional transgenic

Advantages: introduction of sporadic cancer, real tumor microenvironment, ability to study tumor initiation and development.

Disadvantages: target a limited number of genes, cannot reflect human tumor heterogeneity, complex breeding schemes for generating compound mice.

c. Orthotopic xenograft

Advantages: ability to predict drug response of human patient, reflection of real heterogeneity of human tumor, closely mimic human metastasis, better indication of potential clinical activity of drug.

Disadvantages: expensive, technically difficult, stromal irritation, dissociation of tumor cells from their niche.

Many conventional knockout mice bearing germ line deletions of tumor suppressor genes that play a key role in human lung cancer, for instance retinoblastoma (Rb) and Wilms tumor- 1 (Wt-1) genes, resulted in embryonic or perinatal lethality [91]. Conventional knockout mice with embryonal viable tumor suppressor lesions often have a limited life span and they can develop a wide tumor spectrum, because only a small fraction of it becomes lung tumors. An affirmed strategy for generating somatic mouse models for sporadic lung cancer makes use of site-specific recombinase to introduce genetic lesions inside lung tissue cells of adult mice. Currently, Cre/loxP strategy is the most commonly used system in mice to produce strains with conditional alleles. A different application of the Cre/LoxP method, by placing a LoxP-Stop-LoxP (LSL, a transcription stop, flanked by two LoxP sites) DNA segment upstream of an oncogene, enables one to control conditional activation of oncogenes. Cre expression provides for somatic delivery and tissue-specific expression. Somatic administration of engineered Adeno-Cre or Lenti-Cre viruses (recombinant viruses expressing Cre- recombinase) via intranasal or intratracheal route can be used as a specific strategy to introduce Cre recombinase inside a broad range of lung epithelial cells. The tumor multiplicity can be easily controlled by the amount of virus administered. This, together with the use of tissue-specific promoters that regulate Cre recombinase expression, this technique is really versatile.

The major difference using Lentivirus in respect of the Adenovirus:

- Lentiviral DNA can stably integrate into the genome of dividing and nondividing host cells, and lead to long-term expression of the Cre transgene [92].
- Adenoviral DNA does not integrate into the genome of host cells and cannot replicate during cell division [93]

Studies demonstrated that the infection efficacy of adenovirus is higher (nearly 100%) than that of lentivirus (30%). Despite all, Lentiviral Cre vectors remain valuable tools for the somatic onset of lung cancer in Cre/lox mice models. For instance, intratracheal administration of lentiviral Cre-expressing vectors into lungs of Kras LSLG12D/+; Trp53floxflox mice resulted in the development of between 5 and 20 tumors per single lung [94]. Since the lentivirus integrated stably into genome, it was possible to use the integration site as an ideal lineage marker that definitely linked primary tumors to their related metastases (Figure 1) (Figure 8).

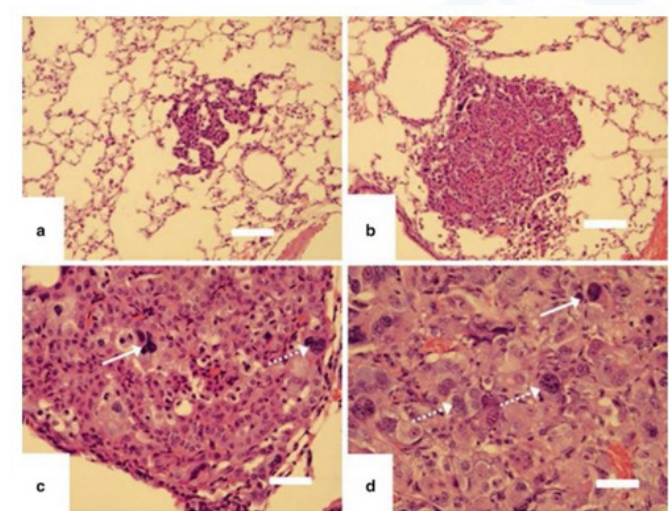


Figure 8: Representative lung tumor lesions from Trp53floxflox : krasLSL-G12W+ mice, after ad-cre infection. (a) Atypical adenomatous hyperplasia occurred 3 weeks post-infection (p.i.) (scale bar+25um). (b) Adenoma lesion found 6 weeks p.i. (scale bar= 25um). (c,d) More advanced adenocarcinoma lesions developed at 3 monts p.i. Tumors cells contain pleomorphic nuclei (white arrow) and giant cells (dotted arrow) (c) scale bar = 15um and (d) scale bar =10 um [94].

One should however be aware of a potential problem that might arise by the use of regular, lung tissue specific, transgenes. Continuous high levels of somatically expressed Cre recombinase can lead to significant genotoxicity in vivo [95]. The use of Adeno Cre virus does circumvent this problem, since the adenoviral Cre recombinase is only transiently active in all infected cells. In case of Lentiviral Cre one should hence use a floxed Cre recombinase [96] in order to guarantee a self-inactivating Cre activity that renders it a de facto transient expression. In another study, lentiviral vectors have been designed containing Cre ER T2 coupled with luciferase and

mStrawberry fluorescent proteins. These vectors contain a single actin (CAG) promoter flanked by inverted mutant loxP sites, which drives CreER T2 expression. After Cre recombinase activation through administration of tamoxifen, the promoter inverts and locks into opposite orientation and consequently expresses bioluminescent and fluorescence reporter proteins while Cre expression itself is inactivated. Then, initiated tumors in KrasLSL- G12D/+; Trp53floxflox mice could be visualized by bioluminescence imaging without the need of an additional reporter transgene [97]. A powerful attribute of ER- inducible systems is that removal of hormone can reverse the activity of ER-fusion proteins. This method was used to engineer Trp53KI/KI mice in which both endogenous Trp53 alleles were replaced by a fused conditional variant Trp53ERTAM (or Trp53KI). When Trp53KI/KI mice underwent tamoxifen treatment or withdrawal, their Trp53 status switched between wild-type and null activity, respectively. Inhalation of Ad-Cre in compound KrasLSL- G12D/+; Trp53KI/KI mice resulted normally in multiple lung tumors. At 8 weeks after Ad-Cre application, Trp53 wild-type function was restored by treating mice with tamoxifen, which then led to a significant decrease in the number of high-grade tumors [98]. This, thus clearly showed the importance of Trp53-mediated tumor suppression in lung cancer driven by oncogenic Ras activity. It however also shows that (re)introduction of Trp53 wild-type levels does not prevent the growth of early, low-grade Ras dependent-tumors. The above mentioned techniques of generating somatic lung cancer have led to the creation of distinct models for various lung cancer subtypes.

Mutations in the K-Ras gene are present in approximately 30 percent of adenocarcinomas and are generally associated with a poor prognosis [91]. The K-Ras oncogene encodes a family of membrane-bound guanosine triphosphate- (GTP-) binding proteins that are involved in cell proliferation, migration, and apoptosis. The most common K-Ras mutations are in the form of point mutations on exons 12 and 13, typically resulting in constitutive activation of RAS [99] interestingly; cases of NSCLC exhibiting K- Ras mutations are predominately resistant to the EGFR inhibitors, erlotinib, and gefitinib [100]. In addition to K-Ras, p53 is a well-established predictive and prognostic marker for NSCLC. Loss of the tumour suppressor gene, p53, leads to mitotic abnormalities during cellular development resulting in highly proliferative cells [17]. Transversions along the p53 gene are found in almost all human lung cancer tissues and have implicated p53 as a key molecular marker for lung cancer [101]. A comprehensive meta- analysis of the role of p53 as a prognostic factor for lung cancer survival revealed that mutated or inactive p53 was shown to be associated with a poor survival [102].

NSCLC can be subdivided into adeno-, squamous cell, bronchoalveolar, and large-cell carcinoma and account for about 80 % of all lung cancers. Somatic mutations in KRAS, BRAF, EGFR, LKB1, RAC1, NF KB, and TRP53 occur frequently in human NSCLC and have been subsequently

introduced in mice [103]. Especially the somatic introduction of Kras mutation has so far been widely used as the basis of many mouse models for NSCLC.

The phenotype of the latter mouse model is in contrast with the more progressed adenocarcinomas found in other conditional mouse models with different Kras mutations, which makes that this model can be easily used for early stages of NSCLC [104]. The practical use of Kras-mediated lung cancer models and its importance for translational research was underlined by the findings that gene expression profiles from murine Kras2- mediated lung cancer and human lung adenocarcinomas proved to be closely related [105]. About 18 % of all lung tumors are classified as Small Cell Lung Cancer (SCLC) [7]. Among the specific characteristics of SCLC are a high proliferative rate and early metastatic behavior, which results in poor prognosis with more than 95 % mortality .SCLC development is strongly linked to tobacco smoking and arises from neuroendocrine (NE) cells [96]. In stark contrast to NSCLC, spontaneous or chemically induced murine lung cancer never developed neuroendocrine carcinomas. Frequent inactivation of both TRP53 and RB1 has been reported in human SCLC and prompted the generation of a somatic SCLC mouse model with conditional alleles for Rb1 and Trp53. Intratracheal Ad-Cre administration in Trp53fl ox,fl ox;Rb1fl ox,fl ox mice led after 6-8 weeks to the growth of hyper plastic NE cellular foci, which rapidly became dysplastic and grew into fully invasive SCLC after an additional 3-5 months [106].

This presentation of mouse models for both NSCLC and SCLC that are well defined and currently in use for preclinical studies. Although the main emphasis is on the genetically modified (somatic) mouse models of lung cancer, we certainly do not want to lessen the importance of using primary human lung cancer cells in orthotopic transplantation studies. The latter studies are very valuable since one has to realize that almost all somatically induced murine lung tumors are genetically very similar to human lung tumors, as has been shown by genome-wide comparison and characterization of all genetic variations in individual tumors. Still, important differences remain. Human lung cancers, whether they are NSCLC or SCLC, have almost always a much higher degree of genetic modifications than murine lung cancers have. A reason for this might be that the whole scale of genetic modifications is limited by the relative short time period of tumor development, which is allowed during the limited life span of a mouse. Another important aspect remains the differences in cellular organization of lung tissue that exists between mouse and man. All these major differences in epithelial organization and homeostasis of the pulmonary tissue certainly influence the onset of different murine lung cancer types, as we clearly showed in the case of SCC. Finally, we want to emphasize that there are not yet convincing mouse models that address the important role of genome-wide epigenetic changes, which most likely play an important role not only during lung cancer growth and maintenance

but also in its response against (cytotoxic) therapies. Many of the abovementioned problems and differences can be addressed by developing new or further refining existing mice models for lung cancer so that their role and use in preclinical research will further increase.

Aim of Study

Normal cells became tumor cells through deregulation of multiple pathways. There are some pathways that are altered in many tumors and RB and p53 pathways are one of the most important. These proteins are regulated during carcinogenesis by a phosphorylation mechanism. In vivo and in vitro data have demonstrated that Pin1 is involved in many aspects of cell cycle control and a plethora of protein targets have now been discovered many of which are involved in the cell cycle control. Different observations indicated that Pin1 may serve as a mediator of malignant behavior in lung cancer and suggested that the inhibitory targeting of Pin1 might be incorporated into novel lung cancer therapies. However, it is not known whether Pin1 would affect actual cellular growth or tumorigenic properties in lung cancer. The project's focus will be studying the role of Pin1 in controls lung cancer tumor cell proliferation. We use a recombinant lentivirus expressing Cre recombinase (LentiCre) to induce HaPin1 murine model. Tumour-associated cell cycle defects are common in eukaryotic cells [107], they induce unscheduled proliferation as well as genomic and chromosomal instability.

To validate the oncogenic potential of Pin1 in lung cells, we propose investigated the biological effect of the overexpression of Pin1 in a conditional mouse model. To do that we are going to use a validated method of intratracheal LV injection to specifically induce lung cells tumor growth. We genotyped and selected mice engineered for p53 and KRAS, obtaining a perfect model to study the function of a Pin1 mutated gene. A specific part of the project will be dedicated to the LV production, titration and efficiency evaluation conducted through transfection process on 293FT cells and rt-pcr technique. Once ultraspin- dried and isolated the vectors (HIV lentiviruses) particular attention has been given for the intratracheal LV injection on mice models. The onset of human lung cancer occurs through sequential mutations in oncogenes and tumor suppressor genes. Mutations in K-Ras and p52 play a prominent role in human non-small cell lung cancer. Mice genetically engineered obtained through this technique allowed to create models bearing a mutated form of Pin1 completed by Cre-Lox technique.

Mutations in Pin1 play a prominent role in human non-small cell lung cancer [108].

Aim of Study (Italian Language)

Le cellule normali diventano tumorali attraverso una deregolazione di numerosi pathways. Molti di questi sono alterati in diversi tumori, I pathways di RB e p53 sono tra I piu' imoportanti. Queste proteine sono regulate durante la

carcinogenesis da meccanismi di fosforilazione. Dati sia in vivo che in vitro hanno dimostrato che pin1 è coinvolto in molti aspetti del controllo del ciclo cellulare insieme a diverse protein target. Differenti osservazioni indicano che Pin1 potrebbe fungere da mediatore nel comportamento maligno del tumore al polmone, suggeriscono inoltre che il targeting e l'inibizione di Pin1 potrebbe essere incorporate in diverse nuove terapie contro questo tipo di tumore. Comunque, non è ancora conosciuto se Pin1 potrebbe avere effetti sulla crescita cellulare e sulle proprietà tumorogeniche del tumore al polmone. Il progetto è incentrato sullo studio del ruolo di Pin1 nel controllo della proliferazione delle suddette cellule tumorali. Per far questo abbiamo utilizzato un Lentivirus esprimente la ricombinasi Cre per indurre un modello murino HaPin1. In cellule eucariotiche sono molto comuni tumori associate a difetti del ciclo cellulare [107], questi inducono una proliferazione incontrollata provocando instabilità sia genomica che cromosomiale. Per validare il potenziale oncogenico di Pin1 nelle cellule polmonari, abbiamo investigato l'effetto biologico dell'overespressione di Pin1 in un modello condizionale murino.

Il metodo validato e scelto per questo obiettivo è stata l'infezione intratracheale di Lentivirus al fine di indurre con precisione la crescita di cellule tumorali nei Polmoni dei modelli utilizzati. Abbiamo svolto questi esperimenti su topi ingegnerizzati selezionati e genotipizzati per p53 e Kras, ottenendo così un perfetto modello di studio per il gene Pin1 mutato. Una specifica parte del progetto è dedicata alla produzione di Lentivirus HIV, alla loro titolazione e valutazione della loro efficienza, condotta attraverso processi di trasfezione su cellule 293FT e tecniche di rt-pcr. Una volta aver ultracentrifugato ed isolato i vettori (Lentivirus HIV), particolare attenzione è stata data alle iniezioni intratracheali di LV sui modelli murine. L'insorgenza del cancro del polmone umano avviene attraverso mutazioni sequenziali in oncogeni e geni oncosoppressori. Le mutazioni in K-Ras e p52 svolgono un ruolo di primo piano nello human non-small cell lung cancer. I topi geneticamente ingegnerizzati, ottenuti attraverso la tecnica di ricombinazione Cre-Lox, hanno consentito di creare nuovi modelli che portano una forma mutata di Pin1. Queste mutazioni su Pin1 giocano un ruolo primario nello sviluppo dello human non-small cell lung cancer [108]. I suddetti modelli possono essere utilizzati come nuovi modelli di studio per il tumore al polmone. Il trasporto di Cre ricombinasi nelle cellule epiteliali polmonari mediato da lentivirus ha dato luogo a una elevata insorgenza di tumori e metastasi. Questi modelli ci permetteranno di studiare i vari step coinvolti nell'iniziazione e progressione del tumore permettendoci di affrontare questioni come la cellula di origine, e il ruolo delle cellule staminali tumorali nel mantenimento di questi tumori.

Materials and Methods

Lung cancer conditional model

Transgenic mice (TG) are animals that have had a foreign

gene deliberately inserted into their genome. The mice we used for this project were created by the micro-injection of DNA into the pronuclear of a fertilized egg which was subsequently implanted into the oviduct of a pseudo pregnant surrogate mother. This results in the recipient animal giving birth to genetically modified offspring. The progeny are then bred with other transgenic offspring to establish a transgenic line. But the transgenic mice with the combination of all the target genes (p53LoxP and LsLKCRASG12D) of interest are not commercially available, and therefore a certain number is required to:

- Maintenance of breeding colonies (heterozygous x wild-type)
- Maintenance of transgenic colonies p53LoxP heterozygous x heterozygous to generate p53LoxP KO mice p53LoxPKO x LsLKCRASG12D to generate p53LoxP / LsLKCRASG12D double heterozygous
- Generation of inducible double transgenic mice p53LoxP / LsLKCRASG12D double heterozygous x p53LoxPKO (KP model)

We would generate a pilot study to demonstrate the effect of Pin1 in KRASG12D, p53LoxP and double TG mice on lung tumor development. To do that, we need to have a minimum number with a statistical good power. Considering positive and negative variables in molecular tests, we have planned to collect 5 samples per time point. This number included the possibility to lost positive data during the entire study process (i.e. death of animal for different causes, variability samples collection process such as fixation, possible comorbidity of lung related disease or molecular variability). We have to inject Lentiviral CRE, Lentiviral CREPin1, Lentiviral CREPin1mut to generate KO mice with or without overexpression of Pin1. Based on published results [17], we will collect tissues at different stage of tumor development as follow:

2, 4, 6, and 9 = 4 time points

5 mouse/time point = 20 mice

20 mice/lentivirus = 60 mice

60 mice wild type - 20 injected with Lentiviral CRE, 20 injected with Lentiviral CREPin1, 20 injected Lentiviral CREPin1mut

60 mice p53LoxPKO - 20 injected with lentiviral CRE, 20 injected with Lentiviral CREPin1, 20 injected Lentiviral CREPin1mut

60 mice LsLKCRASG12D - 20 injected with lentiviral CRE, 20 injected with Lentiviral CREPin1, 20 injected Lentiviral CREPin1mut

60 mice p53LoxPKO / LsLKCRASG12D heterozygous - 20 injected with lentiviral CRE, 20 injected with Lentiviral CREPin1, 20 injected Lentiviral CREPin1mut. In the following table (Table 3) are resumed all the characteristics of each genetic group.

Table 3: Scheme representing the specific number of mice for each genetic type, and lentiviral treatment induced.

	Mice Injected	Mice Injected	Mice Injected	#Total
KRASG12D	2 months old: 5	2 months old: 5	2 months old: 5	15
	4 months old: 5	4 months old: 5	4 months old: 5	15
	6 months old: 5	6 months old: 5	6 months old: 5	15
	9 months old: 5	9 months old: 5	9 months old: 5	15
#Total	20	20	20	60
p53LoxP	2 months old: 5	2 months old: 5	2 months old: 5	15
	4 months old: 5	4 months old: 5	4 months old: 5	15
	6 months old: 5	6 months old: 5	6 months old: 5	15
	9 months old: 5	9 months old: 5	9 months old: 5	15
#Total	20	20	20	60
double TG KRASG12D + p53LoxP	2 months old: 5	2 months old: 5	2 months old: 5	15
	4 months old: 5	4 months old: 5	4 months old: 5	15
	6 months old: 5	6 months old: 5	6 months old: 5	15
	9 months old: 5	9 months old: 5	9 months old: 5	15
#Total	20	20	20	60
wt	2 months old: 5	2 months old: 5	2 months old: 5	15
	4 months old: 5	4 months old: 5	4 months old: 5	15
	6 months old: 5	6 months old: 5	6 months old: 5	15
	9 months old: 5	9 months old: 5	9 months old: 5	15
#Total	20	20	20	60
#Total	80	80	80	240

General breeding strategy

For trio breeding, one heterozygous male will be mating with two heterozygous females at a time. Females will give birth to no more than six litters of pups, while study males will be used up to the age of 1.5 year without a specified number of mating. Pregnant females are placed in separate cages with commercially nesting material so that they have their litters undisturbed and newborn mice will be weaned after 21 days. Accurate records are maintained in a breeder notebook and on the back of each cage card. Information includes identification of the line or strain, sequential numbering of litters with birth date of each litter, number of pups born, date of weaning, final number of female and male pups produced, comments on animal pregnancies and health status, etc. Animals will be tail clipped for genotyping. Animals will be identified by toe clipping if clipped before 1 week of age which does not cause any bleeding or discomfort to the animal or by ear punch if the animals are older than 7 days of age. The toe clipping is the method of identification of all my active protocols and I would like to follow the same numbering sequence. Specifically, the procedure will be performed in the biological safety cabinet on a sterile diaper. The toe or tail of the animal will be swabbed with betadine and the toe will be clipped with a sterile pair of microdissection spring scissors, while the tail is clipped with a sterile razor blade. A piece of tail no larger

than 5 mm and a toe of no more than 3 mm will be collected from each mouse for DNA extraction and genotyping. Ear punching will be performed with a sterile ear punch.

Lentiviral injection

The protocol in use was adapted from [17]. Mice between 6 and 12 weeks are anesthetized by intra-peritoneal injection of 2-2-2 Tribromoethanol (Avertin, Sigma Aldrich T48402) at room temperature (0.4 mg g⁻¹ body weight for females and 0.45 mg g⁻¹ body weight for males). Full anesthesia is ensured by the lack a toe reflex. The mouse is placed on a platform so that it is hanging from its top front teeth on the bar. The mouse is pushed towards the bar so that the chest is vertical underneath the bar (perpendicular to the platform). The Fiber-Lite Illuminator is directed to shine on the mouse's chest, in between the front legs. An exel Safelet IV catheter for the infection procedure is used. To ensure that the needle does not become exposed and impale the mouse, the needle is hold on the square part of with the thumb and the index finger, and using the middle finger, the catheter is pushed over the end of the needle completely. The tongue is pulled out with a flat forceps and the trachea is located by peering into the mouth to look for the white light emitted from it. The catheter is positioned over the white light emitted from the opening of the trachea and slide into the trachea until the top of the catheter

reaches the mouse's front teeth. The proper placement of the catheter in the trachea can be confirmed by visualizing the white light shining through the opening of the catheter in the mouth. The platform, mouse and catheter are then moved into the bio safety hood. The virus is injected directly into the opening of the catheter to ensure the entire volume is inhaled.

The mice will be given meloxicam 1-5 mg/kg sub cutaneous (SC) at the end of surgery before they wake up. They will be monitored at least every 15 minutes until they have fully recovered, are awake and can move freely about the cage, before being returned to their home cage. They will be monitored at least once daily for the duration of the study.

Delivery of Lentivirus using the intratracheal infection method

Protocols to determine the recombination efficiency of the KrasLSL-G12D and p53fl alleles can be found on the Jacks Lab website (http://web.mit.edu/jacks-lab/protocols_table.html). This is the specific protocol in use to deliver lentivirus into mice trachea, to induce a tumor development specifically in the animal lungs.

Reagents

a. 2-2-2 Tribromoethanol (Avertin, Sigma Aldrich T48402)

Avertin Stock (1.6 g/ml)—Add 15.5 ml tert-amyl alcohol to 25g of avertin. Stir overnight to dissolve. Stable at room temperature (18-25 °C) for approximately 1 year.

Avertin Working Solution (20 mg/ml)—Dilute avertin stock in PBS, stir overnight, and protect from light. Sterilize by passing solution through a 0.22 µm filter. Aliquots may be safely stored at 4 °C in the dark for approximately 4 months.

b. Bleach

c. Lentivirus-Cre (Three PCDH plasmid transfection systems: containing CRE, HAPIN1 and HAPIN1 S67E sequences). Lenti-Cre are stored at -80 °C (viruses are going to be keep on ice prior to infection). Equipment

d. Bottle top vacuum filter (.22 µM, 150 ml)

e. Scale

f. Needles

g. Syringes (1 ml)

h. Flat forceps

i. Exel Safelet IV catheters (22 gauge, 1 inch)

j. Intubation platform and Fiber-Lite Illuminator - For IT administration, set up the platform and light source on a flat surface near the biosafety hood. Insert the catheter into the trachea outside of the hood, and then move the mouse into the biosafety hood to inhale the virus. A sharps waste container is also required for the proper disposal of the needles from the Exel Safelet IV Catheter.

k. Latex gloves filled with warm water

Procedure

Virus Preparation. Preparation and administration of viruses should occur in a biosafety hood and follow all guidelines for biosafety level 2 research.

Avertin Administration. Anesthetize mice via intra-peritoneal injection of room temperature 20 mg ml⁻¹ avertin (use 0.4 mg/g body weight for females and 0.45 mg/g body weight for males). Confirm the mice are fully anesthetized by ensuring that they lack a toe reflex. Administering the correct amount of avertin is crucial to successfully delivering the virus.

Intratracheal infection method.

- i. Place mouse on the platform so that it is hanging from its top front teeth on the bar.
- ii. Push the mouse towards the bar so that the chest is vertical underneath the bar (perpendicular to the platform).
- iii. Direct the Fiber-Lite Illuminator to shine on the mouse's chest, in between the front legs.
- iv. Prepare the Exel Safelet IV catheter for the infection procedure. To ensure that the needle does not become exposed and impale the mouse, hold the square part of the needle with one's thumb and index finger, and using one's middle finger, push the catheter over the end of the needle completely and continue to hold the catheter in place during the infection protocol.
- v. Using the Exel Safelet IV catheter, open the mouth and gently pull out the tongue with the flat forceps.
- vi. Locate the opening of the trachea by peering into the mouth and looking for the white light emitted from the trachea.
- vii. While holding the Exel Safelet IV catheter vertically, position the catheter over the white light emitted from the opening of the trachea, and allow the catheter to slide into the trachea until the top of the catheter reaches the mouse's front teeth. There should be no resistance while inserting the catheter into the trachea.
- viii. While stabilizing the Exel Safelet IV catheter with one hand, remove the needle from the mouth. Prior to removing the needle, the mouse cannot breathe through the catheter. Once the Exel Safelet IV catheter has been inserted into the trachea, promptly remove the needle to allow the mouse to breathe through the catheter.
- ix. The proper placement of the catheter in the trachea can be confirmed by visualizing the white light shining through the opening of the catheter in the mouth.
- x. Move the platform, mouse, and catheter into the bio safety hood.
- xi. Pipette the virus directly into the opening of the catheter to ensure the entire volume is inhaled.

- xii. If the catheter is correctly inserted into the trachea, the mouse will begin inhaling the virus immediately. Once the virus is no longer visible in the opening of the catheter, wait a few seconds for the entire volume to travel down the catheter before removing the catheter from the trachea and disposing of it in 50% bleach.

Tissue Harvesting

Mice are euthanized by CO₂. Euthanasia is confirmed by cervical dislocation. In particular, littermates of wild-type, heterozygous, and knockout mice are euthanized by CO₂ (7 days old or greater) or decapitation (under 7 days of age) for tissue harvesting at different time points at 2, 4, 6 and 9 months. Euthanasia of 7 days old or greater mice will be confirmed by cervical dislocation. Lung tumors, brain, breast, heart, kidney, liver, spleen, spinal cord, testis, ovaries, peripheral blood, skeletal muscle, skin, and bone marrow will be collected from each animal. Part of the tissue at each time point will be snap frozen for molecular biological experiments including protein, DNA, and RNA analysis or fixed for histological analysis.

Genotyping mice (P53 and KRas)

DNA Isolation from Tails - Proteinase K Method

Protocols to isolate DNA from mice tails can be found on the Jacks Lab website: http://jacks-lab.mit.edu/protocols/dna_isolation_proteinase_k_method (The Jacks Lab n.d.)

- Each tail should be in a clean eppendorfs tube.
- Add 500µl of tail lysis buffer containing Proteinase K (PK) to each tube.
- Incubate tail samples in 50-60°C water baths overnight.
- Add 250µl saturated (6M) NaCl to each tube.
- Shake tubes vigorously (~20 times) and incubate tubes on ice for 10 minutes.
- Spin tubes on low speed at 4°C for 10 minutes.
- Remove supernatant and place into a clean eppendorfs.
- Add 650µl isopropanol and invert to mix. Incubate tubes at room temperature for 15 minutes.
- Recover DNA by centrifuging, max speed, 10 minutes at room temp.
- Place tubes inverted on bench and allow air-drying 5 minutes.
- Add 200µl of TE pH 7.5 or sterile water to each tube. Incubate in 50-60°C water baths for 10 minutes. Resuspend pellet by pipetting up and down several times.

PCR analysis

Polymerase chain reaction, or PCR, is a technique to make many copies of a specific DNA region in vitro (in a test tube rather than an organism). Like DNA replication in an organism, PCR requires a DNA polymerase enzyme

that makes new strands of DNA, using exist strands as templates. The DNA polymerase typically used in PCR is called Taq polymerase, after the heat-tolerant bacterium from which it was isolated (*Thermus aquaticus*). *Thermus aquaticus* lives in hot springs and hydrothermal vents. Its DNA polymerase is very heat-stable and is most active around 70°C (a temperature at which a human or *E. coli* DNA polymerase would be nonfunctional). This heat-stability makes Taq polymerase ideal for PCR. High temperature is used repeatedly in PCR to denature the template DNA, or separate its strands. Like other DNA polymerases, Taq polymerase can only make DNA if it is given a primer, a short sequence of nucleotides that provides a starting point for DNA synthesis. In a PCR reaction, the experimenter determines the region of DNA that will be copied, or amplified, by the primers she or he chooses. PCR primers are short pieces of single-stranded DNA. Two primers are used in each PCR reaction, and they are designed so that they flank the target region (region that should be copied). That is, they are given sequences that will make them bind to opposite strands of the template DNA, just at the edges of the region to be copied. The primers bind to the template by complementary base pairing. When the primers are bound to the template, they can be extended by the polymerase, and the region that lies between them will get copied. Both primers, when bound, point "inward" - that is, in the 5' to 3' direction towards the region to be copied. Like other DNA polymerases, Taq polymerase can only synthesize DNA in the 5' to 3' direction. When the primers are extended, the region that lies between them will thus be copied.

PCR primers generally range in length from 15 to 30 bases and are designed to flank the region of interest. Primers should contain 40-60% (G+C), and care should be taken to avoid sequences that might produce internal secondary structure. The 3'-ends of the primers should not be complementary to avoid production of primer-dimers. Primer-dimers unnecessarily deplete primers from the reaction and result in an unwanted polymerase reaction that competes with the desired reaction. Avoid three G or C nucleotides in a row near the 3'-end of the primer because this may result in nonspecific primer annealing, increasing synthesis of undesirable reaction products. Ideally, both primers should have nearly identical melting temperatures (T_m) so that the two primers anneal althroughly the same temperature. The annealing temperature of the reaction depends on the T_m of the primer with the lowest T_m. In order to check p53 and kras genes, we used GoTaq® G2 Flexi DNA polymerase kit, which contains GoTaq® G2 Flexi DNA Polymerase, 5X Green GoTaq® Flexi Buffer and 25mM MgCl₂. The enzyme is supplied in a proprietary formulation containing 50% glycerol with buffers designed for enhanced amplification. The enzyme is a full-length form of Taq DNA polymerase that exhibits 5'→3' exonuclease activities. It is derived from bacteria and his concentration is 5u/µl.

The 5X Green GoTaq® Flexi Buffer, contains two dyes (a blue dye and a yellow dye) that separate during electrophoresis to indicate migration progress in any

amplification reaction that will be visualized by agarose gel electrophoresis followed by ethidium-bromide staining. In particular, the blue dye migrates at the same rate as a 3-5kb DNA fragment in a 1% agarose gel. The yellow dye migrates at a rate faster than primers (<50bp) in a 1% agarose gel. The dyes absorb at 225-300nm, making standard A260 readings to determine DNA concentration unreliable. Also, the dyes have excitation peaks at 488nm and 600-700nm. The Flexi Buffer also increases the density of the sample, so it will sink into the well of the agarose gel, allowing reactions to be loaded directly onto gels without loading dye. Magnesium Chloride Solution has (25mM) provided to allow users to optimize MgCl₂ concentration according to their individual requirements. Promega has found that 1.25 units of GoTaq® G2 Flexi DNA Polymerase per 50µl amplification reaction are adequate for most amplification. Adding extra enzyme generally does not produce significant increases in yield. However, in some cases, more or less enzyme may be beneficial. The key ingredients of a PCR reaction are *Taq* polymerase, primers, template DNA, and nucleotides (DNA building blocks). The ingredients are assembled in a tube, along with cofactors needed by the enzyme, and are put through repeated cycles of heating and cooling that allow DNA to be synthesized.

The basic steps are:

- I. Denaturation (96°C): Heat the reaction strongly to separate, or denature, the DNA strands. This provides single-stranded template for the next step.
- II. Annealing (55-65°C): Cool the reaction so the primers can bind to their complementary sequences on the single-stranded template DNA.
- III. Extension (72°C): Raise the reaction temperatures so *Taq* polymerase extends the primers, synthesizing new strands of DNA.

This cycle repeats 25-35 times in a typical PCR reaction, which generally takes 2-4 hours, depending on the length of the DNA region being copied. If the reaction is efficient (works well), the target region can go from just one or a few copies to billions. That's because it's not just the original DNA that's used as a template each time. Instead, the new DNA that's made in one round can serve as a template in the next round of DNA synthesis (Figure 9&10). There are many copies of the primers and many molecules of *Taq* polymerase floating around in the reaction, so the number of DNA molecules can roughly double in each round of cycling. This pattern of exponential growth is shown in the image below.

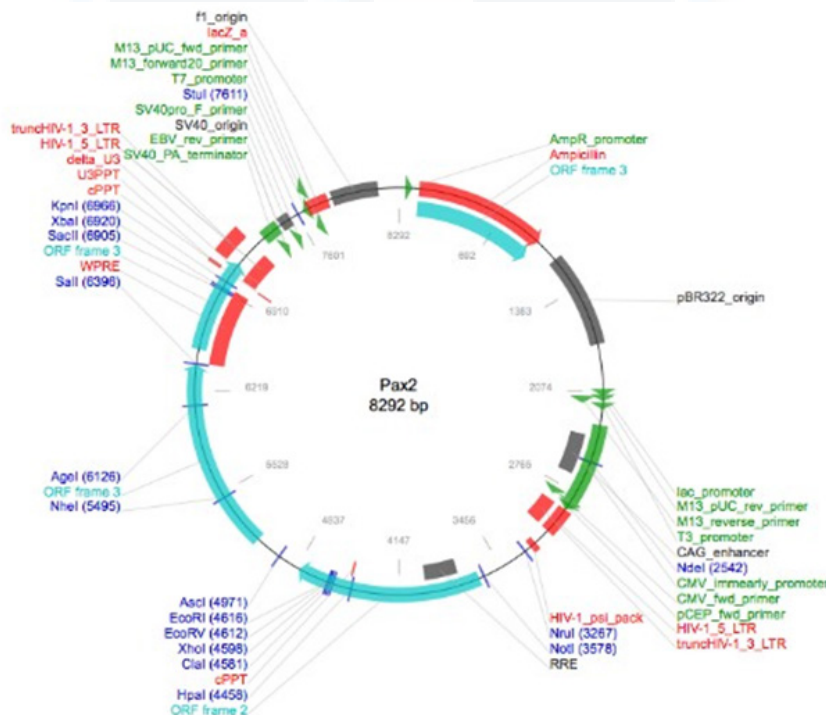


Figure 9: Graphical representation of Pax2 plasmid.

Application of the PCR technique

In a sterile, nuclease-free micro centrifuge tube, combine the following components on ice to prepare the respective pcr reaction mix: (Table 4,5). Centrifuge the reactions in a micro-centrifuge for 5 seconds. After the preparation of samples we used a thermal cycler to begin the polymerase chain reactions (Table 6).

Using gel electrophoresis to visualize the results of PCR

The results of a PCR reaction are usually visualized (made visible) using gel electrophoresis. Gel electrophoresis is a technique in which fragments of DNA are pulled through a gel matrix by an electric current, and it separates DNA fragments according to size. A standard, or DNA ladder, is

typically included so that the size of the fragments in the PCR sample can be determined. DNA fragments of the same length form a “band” on the gel, which can be seen by eye if the gel is stained with a DNA-binding dye (Figure 11&12). A DNA band contains many, many copies of the target DNA region, not just one or a few copies. Because DNA is microscopic, lots of copies of it must be present before we can see it by eye. This is a big part of why PCR is an important tool: it produces enough copies of a DNA sequence that we can see or manipulate that region of DNA.

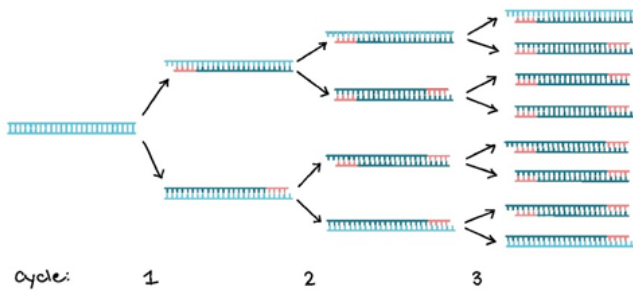


Figure 10: First three PCR cycles schematic representation. Light blue refers to the DNA template; red refers to primer sequence; dark blue refers to the new strand generated.

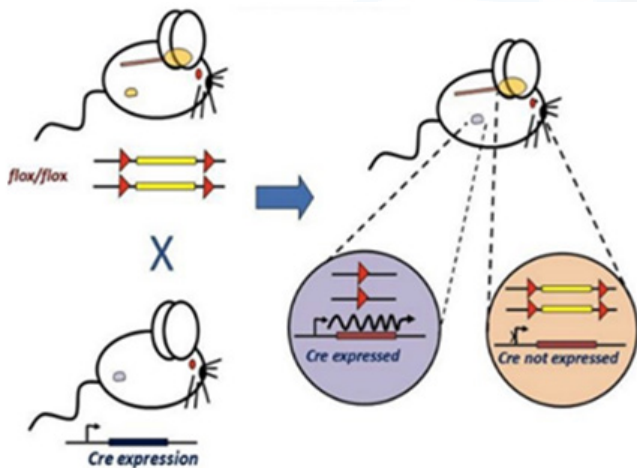


Figure 11: The development of Cre recombinase-controlled (Cre/LoxP) tumor models.

Lentivirus Production and Purification

Lentiviral vectors offer unique versatility and robustness as vehicles for gene delivery. They can transduce a wide range of cell types and integrate into the host genome in both dividing and post-mitotic cells, resulting in long-term expression of the transgene both *in vitro* and *in vivo*. A viral suspension can be routinely prepared with relative ease: a low-titer (10⁶ viral particles/ml) unpurified preparation can be obtained 3 d after transfecting cells with lentiviral vector and packaging plasmids.

This protocol describes how to prepare, purify and titrate lentiviral vectors.

Materials Plasmids and Cells

- a. Human Embryonic Kidney 293 T (HEK-293 T) Cells.

- b. PCDH packaging vector/(Empty Backbone) Express gene of interest under CMV promoter (Add gene) containing genes of interest;
- c. pMD2.G VSV-G envelope expressing plasmid (Add gene);
- d. Pax2 (Add gene).

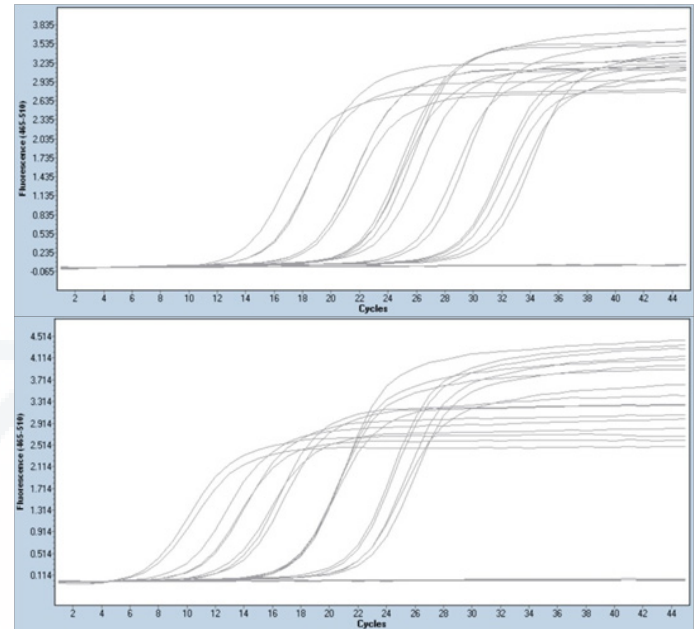


Figure 12: Phases of the Real Time PCR amplification curves for WPRE (a) and GFP (b) markers in PCDH plasmid.

Reagents and Supplies

- I. Penicillin/Streptomycin (Pen/Strep; 10,000 units/mL).
- II. Fetal bovine serum (FBS).
- III. Dulbecco’s modified Eagle media (DMEM) containing high glucose, glutamine, and sodium pyruvate.
- IV. Phosphate-buffered saline (PBS) containing calcium and magnesium.
- V. 0.45 µm filter unit (EMD Millipore).
- VI. 38.5 mL conical thin wall polyallomer ultracentrifuge tubes.
- VII. T175 Culture flasks.
- VIII. Ultracentrifuge (Beckman Coulter).
- IX. Real-time PCR system: Applied biosystems 7500 (Thermo Fisher Scientific).

We prepared complete HEK-293 T media (DMEM with 10% FBS and 1% Pen/strep). Add 100 mL of FBS and 10 mL of Pen/strep to 890 mL of DMEM. Prepare the required amount of plasmid DNA (for each respective plasmid) using a standard plasmid DNA preparation method. DNA must be endotoxin free. The current protocol utilizes the second-generation LV packaging system in which all necessary

genes are separated into three distinct plasmids (the transfer vector, envelope plasmid and packaging plasmid). A third-generation packaging system is also available, in which the necessary genes are further separated into four

distinct plasmids (transfer vector, envelope, and packaging plasmid). Although the third generation system offers increased biosafety, it is also more cumbersome due to the increased number of plasmids.

Table 4: Nuclease-free micro centrifuge tube, combine the following components on ice to prepare the respective pcr reaction mix.

Checking p53		Checking KRAS G12D	
Reagent	Volume:	Reagent	Volume:
DNA (100ng)	2 µL	DNA (100ng)	2 µL
5X Buffer	2.5 µL	5X Buffer	2.5 µL
2.5mM dNTP mix	1 µL	dNTPs 10mM	0.5 µL
100µM Primer fw T008	1 µL	5µM Primer 1	1 µL
100µM Primer rev T009	1 µL	5µM Primer 2	1 µL
dH2O 9.75 µL Taq 0.25 µL TOT 15 µL		5µM Primer 3 1 µL DMSO* 1 µL dH2O 16 µL Taq 0.25 µL TOT 25 µL *To overcome low yield or no yield in amplifications: • Add PCR additives. Adding PCR-enhancing agents (e.g., DMSO) may improve yields.	
Use Promega Green Taq Master Mix One unit is defined as the amount of enzyme required to catalyze the incorporation of 10 nano moles of dNTPs into acid-insoluble material in 30 minutes at 74°C. The reaction conditions are specified below under Standard DNA Polymerase Assay Conditions.			
PCR Primers: T008: 5' cac aaa aac agg tta aac cca g 3' T009: 5' agc aca tag gag gca gag ac 3'		PCR Primers: KRAS 1: 5' gtc ttt ccc cag cac agt gc 3' KRAS 2: 5' ctc ttg cct acg cca cca gct c 3' KRAS 3: 5' agc tag cca cca tgg ctt gag taa gtc tgc a 3'	

Table 5: Centrifuge the reactions in a micro-centrifuge for 5 seconds. After the preparation of samples we used a thermal cyclor to begin the polymerase chain reactions.

PCR Conditions for P53:	PCR Conditions for KRAS:
1. 95°C 3:00	1. 95°C 2:00
2. 95°C 1:00	2. 95°C 0:30
3. 57°C 1:00	3. 61°C 0:30
4. 72°C 0:30	4. 72°C 0:45
5. Goto 2 x35 cycles	5. Goto 2 x34 cycles
6. 72°C 3:00	6. 72°C 10:00

All work should be done in a culture hood using sterile technique. The size (in nucleotide bases) of the genetic material to be packaged in the lentivirus vector will alter the size of the pCDH plasmid, and the corresponding weight of DNA, needed for transfection. To maintain accuracy, determine the molecular weight of the plasmid containing the genetic material of interest and then calculate the total amount (in nano grams) necessary to transfect >6×10¹¹ copies of the plasmid. This can be done easily using an online DNA molecular weight calculator. Seed the T175

flask with HEK-293 T cells. Grow HEK-293 T cells in a T75 starter flask prior to seeding the T175. Once the T75 starter flask is at 90-95% confluence aspirate media from the flask and gently rinse with sterile PBS. Incubate cells with 4mL of dissociation reagent at 37°C for 5 min. Add 6 mL of media containing serum to deactivate the dissociation reagent, and triturate with 25-30 full strokes of a serological pipette to create a single cell suspension. Determine cell number per mL using a hemo cytometer.

Calculate the amount of the single cell suspension needed to seed the T175 flask with 3×10⁷ HEK-293 T cells. Add cells to flask and bring the total volume of the flask to 28 mL with warm (37°C), complete HEK-293 T media. Incubate T175 Flask at 37°C with 5% CO₂ overnight or until 80-90% confluence is reached. We use the FuGENE®HD Transfection Reagent, which is a proprietary mixture of lipids and other components in 80% ethanol, sterile filtered and supplied in sterile glass vials. Before use, allow FuGENE to reach room temperature, and mix briefly by inverting or vortexing. No precipitate should be visible. Successful transfection involves optimizing the FuGENE in terms of DNA ratio, amount of DNA used, complexion time, cells and medium used, etc. To create the complete transfection

mixture, two separate solutions are first prepared, a DNA solution and the transfection solution: dilute DNA to 2µg per 100µl of serum-free medium (Opti-MEM reduced-serum medium) and add an appropriate amount of FuGENE to achieve the proper ratio of reagent to DNA (16µl) and incubate for 20 minutes. Plate cells one day before the transfection experiment so that cells will be approximately 80% confluent on the day of transfection. Prepare the

complete transfection solution by adding the FuGENE solution drop wise to the DNA solution. Vortex vigorously for 1-2 min. Incubate the complete transfection solution at room temperature for 20 min. Add 200µl of complete solution (FuGENE and DNA mixture) to each well of cells to be transfected, and mix gently. There is no need to remove serum or change culture conditions. Incubate for 24 hours at 37°C and 5% CO₂.

Table 6: DNA fragments of the same length form a “band” on the gel, which can be seen by eye if the gel is stained with a DNA-binding dye.

P53	KRAS
<p>Expected Bands:</p> <p>(run gel a long way to discern between the 2)</p> <p>5' Loxp (recombined) = ~590 bp Wt= ~288bp</p> <p>What a gel would look like:</p>	<p>Expected Bands:</p> <p>(run gel a long way to discern between the 3)</p> <p>Wt = ~622bp</p> <p>LSL-cassette = 500bp</p> <p>1 Lox (recombined) = ~650bp</p> <p>What a gel would look like:</p>

The supernatant is collected at 24h post-transfection and again at 48h post-transfection. At the 24-h time point, collect the viral media in a 50 mL polypropylene conical. Replace the media with 28 mL of warm (37°C) complete HEK-293 T media. Spin the collected viral media at 783×g in the RC 6 centrifuge for 5 min to pellet cell debris. Collect the supernatant and store in a fresh tube at 4°C. At the 48h time point, again collect the media and remove debris by centrifugation. Pool all viral media from the 24- and 48-h time points. Filter the viral media through the 0.45µm filter. Split the viral media into two thin wall polyallomer ultracentrifuge tubes. Carefully load the filled ultracentrifugation tubes into the SW32Ti rotor and spin at 80,000 × g for 2 h at 4°C. Remove the supernatant from the viral pellet by carefully aspirating the media from the ultracentrifugation tube. After removing the supernatant, resuspend the viral pellet by gently overlaying the pellet with 10µL of sterile PBS in the conical. Seal the conical tube with parafilm and store at 4°C overnight. After overnight incubation, place the sealed conical on ice. Gently shake the conical on an orbital rotating shaker for 2h. Aliquot the resuspended virus into working aliquots and store at -80°C. The quality of the transfection can be determined by GFP transgene: transfection efficiency can be determined by observing the HEK-293 T cells with a fluorescence microscope.

Lentiviral titration methods

For these studies, we utilized the pCDH-GFP lentiviral vector, which expresses the GFP gene under control of the H1 promoter. To assess the lentiviral titer, the HEK293T (ATCC) cell line was cultured in standard conditions. Briefly, cells (50% confluence, max.3rd passage) were cultured in DMEM medium supplemented with 10% fetal bovine serum (Sigma-Aldrich) and 1% penicillin/streptomycin (Sigma-Aldrich). Experiments were performed in 24-well plates (50,000 cells per well) for 96h. After media changing, lentiviruses obtained according to a previously described protocol were added to wells in different volumes (4 or 2µl). Transduction was performed in the presence of polybrene (5µg/ml, Sigma-Aldrich). After 96h incubation (reducing the contamination from plasmid DNA) at 37°C and 5% CO₂, cells were harvested and DNA was isolated. DNA was extracted from HEK293T cells using a mini column-based DNA isolation kit (A&A Biotechnology; Gdynia, Poland) and stored at -20°C, according to manufacturer’s protocol. High concentration standard samples of plasmid and oligonucleotide DNA were prepared in decimal concentrations to cover all possible measurement ranges.

The concentration of lentivirus was assessed with two pairs of primers: two lentiviral-specific transgene (WPRE

and GFP gene) according to standard procedure. The primers (eGFP: 5'-GGAGCGCACGATCTTCTTCA-3' and 5'-AGGGTGTGCGCCCTCGAA-3'; WPRE 5'-CCGTTGTCAGGCAACGTG-3' and 5'-AGCTGACAGGTGGTGGCAAT-3') were tested in the context of specificity. A detailed analysis and optimization of the reaction protocol were performed to obtain a precise description of the efficiency of individual reactions. The protocol was optimized to eliminate primer-dimer formation even after 45 cycles of amplification or in low DNA content samples. These steps enabled validation of the method and, consequently, more reliable and reproducible results. Additionally, the protocol was performed on a base of the universal SYBR green dye in a mono-color reaction, which makes the method easy to implement in any qPCR platform. We used The Fast Start Universal SYBR Green Master (ROX - Roche) it is a 2×concentrated master mix that contains all the reagents, except primers and template, needed for running real-time DNA detection assays.

The primer concentration and the annealing temperatures analysis were also optimized, thus increasing reaction efficiency with simultaneous elimination, a primer-dimer formation. Concentration of PCR primers used is 0.5M. It is important to always use equimolar primer concentrations. Moreover, the design of the PCR primers determines amplicons length, melting temperature, amplification efficiency, and yield. The optimal PCR conditions to amplify the lentiviral-specific fragment WPRE and GFP were carried out as follows: initial denaturation and polymerase activation (hot start) were performed at 95°C for 5 min without fluorescence acquisition. The signal was detected during another 45 cycles (95°C/10 s, 60°C/10 s, and 72°C/10s). Melting analysis (65-95 °C range, 0.11°C resolution) at the end of the reaction was performed to verify specificity of the product; that analysis indicated $T_m = 84.5^\circ\text{C}$ (WPRE gene) and $T_m = 83^\circ\text{C}$ (GFP). The efficiency of the reaction was no lower than 94.4%. Importantly, this result was repeatable for all samples that were analyzed (in serial dilutions). To detect DNA contamination, always include a negative control in each run. To prepare this control, replace template DNA with PCR- grade water. Standard curves for WPRE and GFP genes were obtained using plasmid carrying WPRE gene and GFP gene. The lentiviral titer was assessed using a qPCR system and SYBR Green Master Mix kit. In particular, we analyzed our lentiviral DNA template: pCDH-CRE, pCDH-Pin1 and pCDH- Pin1mut. All templates (and controls) must be amplified in triplicate.

Histopathological analysis of lung cancer in mice

Important parts of any gross postmortem examination (gross necropsy) are the history of the animal and the description of the findings. This is important for the veterinary pathologist reading your histopathology slides because he has not have seen the animal, and is relying for the background information.

Gather the necessary supplies prior to euthanasia of the animal:

- Dissection board
- Forceps
- Scissors
- Labels for containers
- Fixative
- Collection tubes/cups

Before euthanize the animal according to the standard procedure, it is necessary to briefly assess the condition, behavior, and movement of the animal. Observe and record breathing patterns (e.g., rapid, shallow) as well as ambulatory ability and gait (e.g., limping, circling, tremors). Lay the euthanized mouse carcass in dorsal recumbence on a clean dissection board and using scissors, incise the skin the full length of the ventrum from the anus to the chin, reflecting the skin and incising the abdominal wall, exposing the abdominal viscera, salivary and perpetual/clitoral glands, and cervical and axillary lymph nodes. Cut the rib cage to expose and examine the thoracic viscera by making 2 cuts laterally up each side of the ribcage, then one across, at the top of the sternum, to open a space wide enough to thoroughly examine all the lobes of the lung. Evaluate all organs for abnormalities: specifically find and identify the heart and lungs in the thoracic cavity. Note any color changes, size differences, and missing or misallocated organs. Finally, check the mesentery for enlarged lymph nodes and/or masses.

At this point, the tissues are going to be fixed, processed, embedded and sectioned, following this procedure: the lungs are inflated with fixative; each lobe is separated and laid flat between sponges in labeled cassettes, and fixed, for processing, embedding and sectioning. It is best to label the cassettes using the indelible marker (not a sharpie, the ink of which is soluble in the solvents that are used to process the tissues into paraffin). It is also extremely important to confer with the histo technologist when you deliver the sample so that both of you can determine the correct orientation of the tissues, so that you will receive properly oriented, embedded, sectioned and stained slides to review and photograph. Our fixed tissue sections have been processed and analyzed for immunohistochemical assays by the Fox Chase Facility, which recommended to do not fix for longer than 24 hours in paraformaldehyde or formalin and transfer to 70% alcohol and take to the histology lab for immediate processing, in order to be able to detect non-denatured epitopes easily.

Results

The development of Cre recombinase-controlled (Cre/LoxP) tumor models has allowed for the generation of autochthonous tumors derived from a limited number of somatic cells that become transformed in their natural location, surrounded by a normal tissue microenvironment. By engineering LoxP DNA elements into the mouse genome that either surround ('flox') exons critical to a

tumor suppressor genes function or surround a synthetic 'stop' element ('LSL') inserted in front of an oncogene, investigators can 'turn-off' tumor suppressors or 'turn-on' oncogenes with delivery of Cre recombinase to the appropriate cell types. We have used a described protocol to initiate tumors in conditional genetic model of human non-small cell lung cancer (NSCLC) using the inactivation of oncogenic K-ras in combination with the loss of function of p53 and compensation with overexpression of Pin1 protein administrating lentivirus by intratracheal intubation. To reduce variability related to the LV infection efficiency, we optimize the process of viral titration before start out *in vivo* process.

Results Lentiviral Titration methods

Rt-Pcr

Lentiviral titer can be assessed with the use of qPCR based on the SYBR Green based detection system. To evaluate the lentiviral titer of HEK293T cell line (ATCC), cells were cultured in DMEM medium supplemented with 10% fetal bovine serum (Sigma-Aldrich) and 1% penicillin/streptomycin (Sigma-Aldrich). Lentiviruses obtained according to a previously described protocol were added to wells in different volumes (4 or 2ul). After 96 h incubation (reducing the contamination from plasmid DNA) at 37°C and 5% CO₂, cells were harvested and DNA was isolated. High concentration standard samples of plasmid and oligonucleotide DNA were prepared in decimal concentrations to cover all possible measurement ranges. The number of lentiviral vector copies was calculated by a standard curves for two specific plasmid sequences (WPRES and GFP), and the estimation of absolute DNA titers was achieved by comparing crossing point values derived from DNA samples to those obtained from a standard curve of concentrations of plasmid lentiviral DNA.

The number of copies was calculated according to the following formula:

$$\text{Number of copies} = (X \text{ ng} \cdot 6.0221 \cdot 10^{23} \text{ molecules/mole}) / [(N \cdot 660 \text{ g/mole}) \cdot 10^9 \text{ ng/g}]$$

Where X is the amount of amplicons (ng), N is the Length of dsDNA amplicons, and 660 g/mole is an average mass of 1bp dsDNA. The lentiviral titer is viral particles per mL of supernatant able to transduced target cells (TU/mL). Efficacy was very high and there were no observed relevant primer-dimer fragments during the melting curve analysis in either the WPRES or GFP amplicons. The efficiency of the reaction was no lower than 94.4%. Specifically, the concentration of lentivirus was assessed with two pairs of primers: two lentiviral-specific transgene (WPRES and GFP gene) according to standard procedure. The primers (eGFP: 5'- GGAGCGCACGATCTTCTTCA-3' and 5'-AGGGTGTGCGCCCTCGAA- 3'; WPRES 5'- CCGTTGTCAGGCAACGTG-3' and 5'-AGCTGACAGGTGGTGGCAAT-3') were tested in the context of specificity. This result was repeatable for all samples that were analyzed in serial dilutions: from 1

*10⁻¹ to 1*10⁻¹⁰. Standard curves for WPRES and GFP genes were obtained using plasmid carrying WPRES gene and GFP gene. This rt-pcr has been made for GFP gene in RRL and PCDH plasmids and for WPRES on RRL and PCDH plasmids. Moreover we have been made a rt-pcr for GFP and WPRES in lentivirus containing CRE or CREHAPIN genes. All templates (and controls) were amplified in triplicate.

Elaboration results

As previously described The Cp (Crossing point-PCR-cycle) or CT (Threshold Cycle) value is the cycle at which fluorescence achieves a defined threshold. It corresponds to the cycle at which a statistically significant increase in fluorescence (ΔR_n or non-normalized) is first detected. This concept is the basics for accurate and reproducible quantification using qPCR; the number of cycles needed for the amplification-associated fluorescence to reach a specific threshold level of detection (the CT or Cp value) is inversely correlated to the amount of nucleic acid that was in the original sample. This value always is in the exponential phase of amplification, when amplification is most efficient, and therefore quantification is least affected by reaction-limiting conditions. To obtain a more accurate result, in each reaction was also included a positive control made of DNA extracted from a pull of infected cells. Computing the average rt-pcr crossing point (Cp) we obtained the following results:

GFP in RRL (Table 7), GFP Standard Curve (Figure 13), WPRES in RRL (Table 8), WPRES Standard Curve (Figure 14), GFP in pCDH (Table 9), GFP pCDH standard curve (Figure 15) WPRES in pCDH (Table 10), WPRES pCDH Standard Curve (Figure 16)

Table 7: GFP in RRL.

RRL	Cp			Average
GFP dil -1	17.12	17.51	17.76	17.51
GFP dil -2	21.94	21.26	21.18	21.26
GFP dil -3	17.46	22.67	22.11	22.11
GFP dil -4	23.01	25.56	26.24	25.56
GFP dil -5	29.16	28.87	28.8	28.87
GFP dil -6	30.88	30.20	22.54	30.20
GFP dil -7	31.93	32.09	32.69	32.09
GFP C+	13.60	13.32	17.25	
GFP C-	0.00	0.00	0.00	0.00

Comparing the results obtained from RRL plasmid to results obtained from pCDH plasmid, we decided to conduct our experiment with the preparation of viruses containing the pCDH plasmid, because of the better value of final viral preparation. Starting from these information, we used Cp value to calculate the concentration of Cre and CREHAPIN according to the formula $X=(Y/M)-Q$, referring to the specific values reported in the previous graphs. Specifically, we

will use $y = 2.4661x + 15.56$ ($M=2.4661$ and $Q=15.56$) for the quantification based on GFP, and $y=2.7405x+6.4071$ ($M=2.7405$ and $Q=6.4071$) for the quantification based on WPRE. We have done the analysis in triplicate for two samples to be sure that there were not significant differences. Obtained values are reported in the following tables:

- I. GFP in CRE and CREHAPIN (Table 11). WPRE in CRE and CREHAPIN (Table 12). We apply the formula to each average reported on Table 8&9. To have a precise quantification we considered another important parameter the virus weight, which is fundamental to normalize the value obtained. It is calculated converting the plasmids weight (Da) to micrograms. The number of virus is calculated starting from X value, or concentration, divided for virus weight value, and considering the reaction volume.
- II. GFP in pCDH CRE -> num virus = $5,8 \times 10^4$
- III. WPRE in pCDH CRE -> num virus = $5,3 \times 10^4$
- IV. GFP in pCDH CREHAPIN1 -> num virus = $9,1 \times 10^4$
- V. WPRE in pCDH CREHAPIN1 -> num virus = $5,3 \times 10^6$

Table 8: WPRE in RRL.

RRL	Cp			Average
WPRE dil -1	7.13	5.00	6.68	6.27
WPRE dil -2	10.56	10.88	9.65	10.36
WPRE dil -3	13.63	12.65	13.19	13.16
WPRE dil -4	15.64	15.29	13.63	14.85
WPRE dil -5	18.50	18.49	18.46	18.48
WPRE dil -6	22.01	21.75	21.78	21.85
WPRE dil -7	24.94	23.97	25.01	24.61
WPRE C+	5.00	5.00	5.00	5.00
WPRE C-	0.00	0.00	0.00	0.00

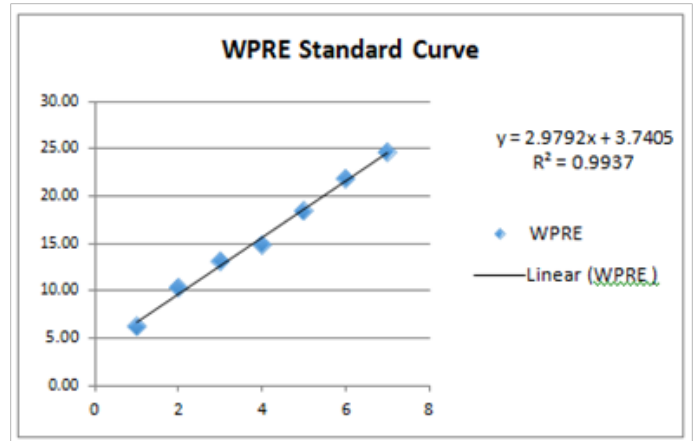


Figure 14: WPRE (RRL) standard curve.

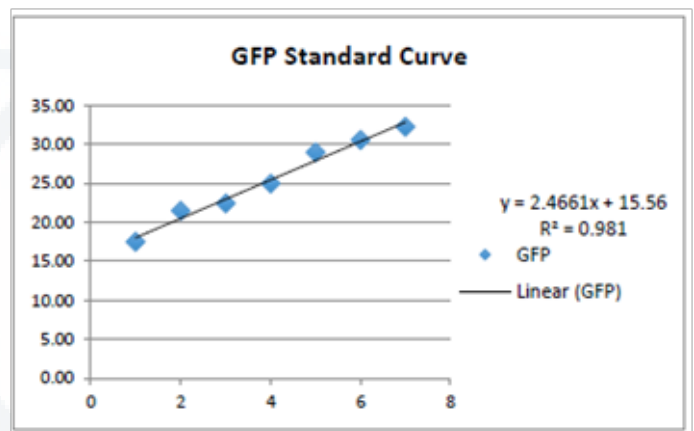


Figure 15: GFP (pCDH) standard curve.

Table 9: GFP in pCDH.

pCDH	Cp			Average
GFP dil -1	8.02	5	7.4	17.46
GFP dil -2	10.95	11.76	11.05	21.46
GFP dil -3	14.78	14.82	13.57	22.39
GFP dil -4	16.74	17.54	17.7	24.94
GFP dil -5	21.18	20.64	20.87	28.94
GFP dil -6	23.44	23.76	24.02	30.54
GFP dil -7	26.02	26.61	26.78	32.24
GFP C+	5	5	5	5
GFP C-	0	0	0	0

The quantity of DNA at the start of the PCR can then be determined by interpolation (o standard curve) of the resulting CT or Cp value in a linear standard curve of values obtained from serially diluted known-amount standards. This standard curve correlates the emitted fluorescence (CT or Cp value) with the initial concentration of the standards used and the final result is achieved by interpolation of the produced fluorescence (CT or Cp value) during the amplification of the sample in this standard curve (Figure 1).

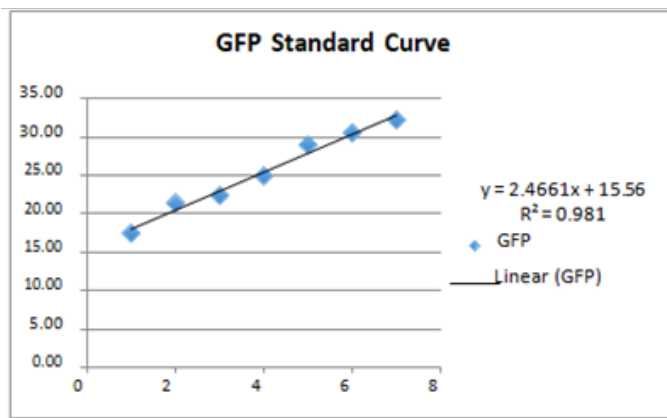


Figure 13: GFP standard curve.

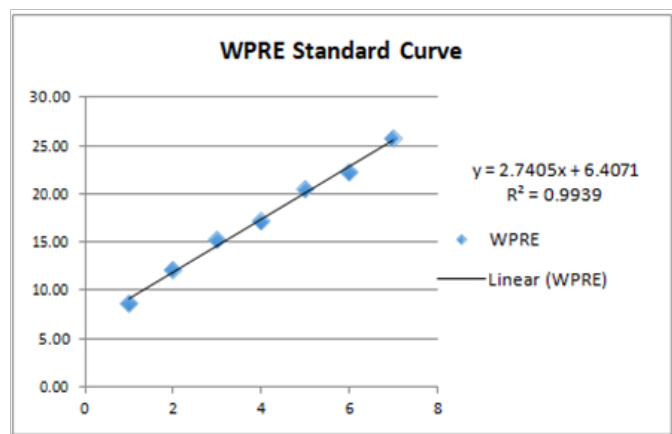


Figure 16: WPRE (pCDH) Standard Curve.

Table 10: WPRE in pCDH.

RRL	Cp			Average
WPRE dil -1	8.84	8.53	8.52	8.63
WPRE dil -2	11.64	12.15	12.51	12.10
WPRE dil -3	15.32	15.18	15.28	15.26
WPRE dil -4	16.94	17.43	17.18	17.18
WPRE dil -5	19.9	20.92	20.62	20.48
WPRE dil -6	23.78	21.72	22.14	22.55
WPRE dil -7	26.24	25.44	25.49	25.72
WPRE C+	5.00	5.00	5.00	5.00
WPR3 C-	0.00	0.00	0.00	0.00

Table 11: GFP in CRE and CREHAPIN.

GFP	Virus Title	Cp			Average
	Sample 1:	pCDH_CRE	27	29.8	28.85
pCDH_CREHAPIN1		26.74	26.21	26.63	26.53
Sample 2:	pCDH_CRE	28.73	29.11	28.12	28.65
	pCDH_CREHAPIN1	28.49	28.3	28.15	28.31
C+		20.92	22.12		21.52
C-		0	0	0	0

Table 12: WPRE in CRE and CREHAPIN.

WPRE	Virus Title	Cp			Average
	Sample 1:	pCDH_CRE	21.22	21.26	21.27
pCDH_CREHAPIN1		24.8	24.93	25.93	25.22
Sample 2:	pCDH_CRE	20.93	21.02	21.16	21.04
	pCDH_CREHAPIN1	25.81	25.72	25.93	25.82
C+		20.92	21.65	19.96	20.78
C-		0	0	0	0

Fluorescence

We confirmed our results obtained from Real Time quantification of GFP with the evaluation of the fluorescence during the process of cells transfection. The HEK293T cells were transfected with a packaging vector expressing a green fluorescent protein (GFP) along with transfer and envelope vectors, and the virus-containing medium being collected at 48hours after transfection was used as the starting materials for the concentration. To measure the titer of the functional virus, the concentrated virus was added to the HEK293T cells, the expression of GFP protein in cells has been seen with a fluorescence microscopy. The concentration of functional virion particles, reflected as the percentage of the cells infected (Figure 17).

The pathological diagnosis on mice model

The pathological status of each animal was first evaluated

macroscopically during the autopsy. It was not easy to see something at the first time points (4&8weeks). Following there are examples of a macroscopic evidence of lung cancer (Figure 18). Fox Chase Facility did the qualitative and quantitative analysis useful to have the characterization of the different stage or histo types (Table 13). To follow changes objectively, we should consider a 4-stage grading system for tumor progression in our NSCLC models. The earliest lesions, designated as Grade 1, are atypical adenomatous hyperplasia (AAH) or small adenomas that feature uniform nuclei and can appear as early as 2-3 weeks post-infection. These earliest lesions can only be identified through careful histological analysis and to see visible lesions on the surface of the lung, investigators should wait until 6-8 weeks after tumor initiation or later. This is the reason of why we were not able to easily detect a lot of adenomatous lesions on our animals (we did just H&E stain). We should do some more specific IHC to better

characterize these early stages on our model. Grade 2 tumors are larger adenomas that have slightly enlarged nuclei with prominent nucleoli and are observed 6-8 weeks post-infection. Some of our case showed an adenomatous status at time point two, or later, sometime associated to AdenoCa diagnosis. However, after 12 weeks we have a relevant incidence of Adenocarcinomas. Adenocarcinomas are classified as Grade 3; they have a great degree of cellular pleomorphic and nuclear atypia and can develop as early as 16 weeks post-infection. Grade 4 tumors are invasive adenocarcinomas that harbor all the cellular

characteristics of Grade 3 tumors but with a higher mitotic index - including irregular mitoses, a distinctive highly invasive stromal reaction (desmoplasia), and invasive edges bordering lymphatic vessels, blood vessels, or the pleura. Grade 4 tumors may develop as early as 18 weeks post-infection in KP animals, but are not observed in K animals. In our study, we have only one case of Grade 4 in KP animals with induced overexpression of Pin1 protein. Following are reported some images representing mice histo type at different time points (Figure 19&20).

Table 13: In this table are reported all the pathological diagnosis.

	wks	LV CRE					LV CRE_HAPin1					LV HAPin 1
K-ras ^{LS} -G12D/+ (K)	22	788	790	826	824	973	838	839	821	909	910	
		2 adenomas	1 adenoma	no tumor seen	no tumor seen	no tumor seen	no tumor seen	no tumor seen	no tumor seen	no tumor seen	no tumor seen	
	16	812	820	817			897	900	906	904	907	
		no tumor seen	no tumor seen	no tumor seen			no tumor seen	no tumor seen	no tumor seen	no tumor seen	no tumor seen	
	8	833	889	890	891	892						44
		no tumor seen	no tumor seen	no tumor seen	no tumor seen	no tumor seen						no tumor seen
	4	34	37	39								
	no tumor seen	lymphoproliferative disease	no tumor seen									
K-ras ^{LS} -G12D/+; p53 ^R /R (KP)	22	786	787	822	827	913	801	792	793	840	841	
		no tumor seen	Lung adenoCA G3	no tumor seen	no tumor seen	2 adenoCA 3 adenoCA 1 early hyperplasia	Multiple lung adenoC As G4	Papillary adenoCA G3	no tumor seen	Adenoma, from a different malignancy	3 adenomas (1 of them papillary)	
	16	828	823	825	813	815	816	716	717	718	721	
		no tumor seen	no tumor seen	Lung adenoCA G3	Lung adenoC A G3	no tumor seen	no tumor seen	no tumor seen	Adenoma, early AdenoCA G2	no tumor seen	Bronchiol or hyperplasia G1	
	8	831	832	40	39	893						42
		no tumor seen	no tumor seen	no tumor seen	no tumor seen	no tumor seen						no tumor seen
	4	48	49	35								
	no tumor seen	no tumor seen	no tumor seen									

To better evaluate the incidence of the pathology on our model, we calculate the percentage of pathological status on each group. Data are reported on the following table (Table

14). The time to tumor development and progression will vary, while survival time will also depend on the amount and type of virus administered to the mice. Decreased survival is

due to a greater growth rate of tumors lacking p53, leading to the more rapid development of a tumor burden that disrupts the normal function of the lungs. Reduced survival after p53 loss could be not due to an increased number of

tumors or metastatic disease. However, survival of mice is also reduced after infection with Lenti-Cre. We estimated that mice infected with roughly 104-105 infectious particles of Lenti-Cre generated 10-100 tumors per mouse.

	LV CRE				LV CRE_HAPin1				LV HAPin1			
	K-ras ^{LSL-G12D/+} (K)		K-ras ^{LSL-G12D/+} ;p53 ^{fl/fl} (KP)		K-ras ^{LSL-G12D/+} (K)		K-ras ^{LSL-G12D/+} ;p53 ^{fl/fl} (KP)		K-ras ^{LSL-G12D/+} (K)		K-ras ^{LSL-G12D/+} ;p53 ^{fl/fl} (KP)	
	Diagnosis	Incidence	Diagnosis	Incidence	Diagnosis	Incidence	Diagnosis	Incidence	Diagnosis	Incidence	Diagnosis	Incidence
22weeks	No tumor	100%	AdenoCA	40%	No tumor	100%	AdenoCA (multiple or papillary)	80%	No tumor	100%	No tumor	100%
16weeks	No tumor	100%	AdenoCA	40%	No tumor	100%	AdenoCA	40%	No tumor	100%	No tumor	100%
8weeks	No tumor	100%	No tumor	100%	No tumor	100%	No tumor	100%	No tumor	100%	No tumor	100%
4weeks	No tumor	100%	No tumor	100%	No tumor	100%	No tumor	100%	No tumor	100%	No tumor	100%

Table 14: Tumor incidence in each group.

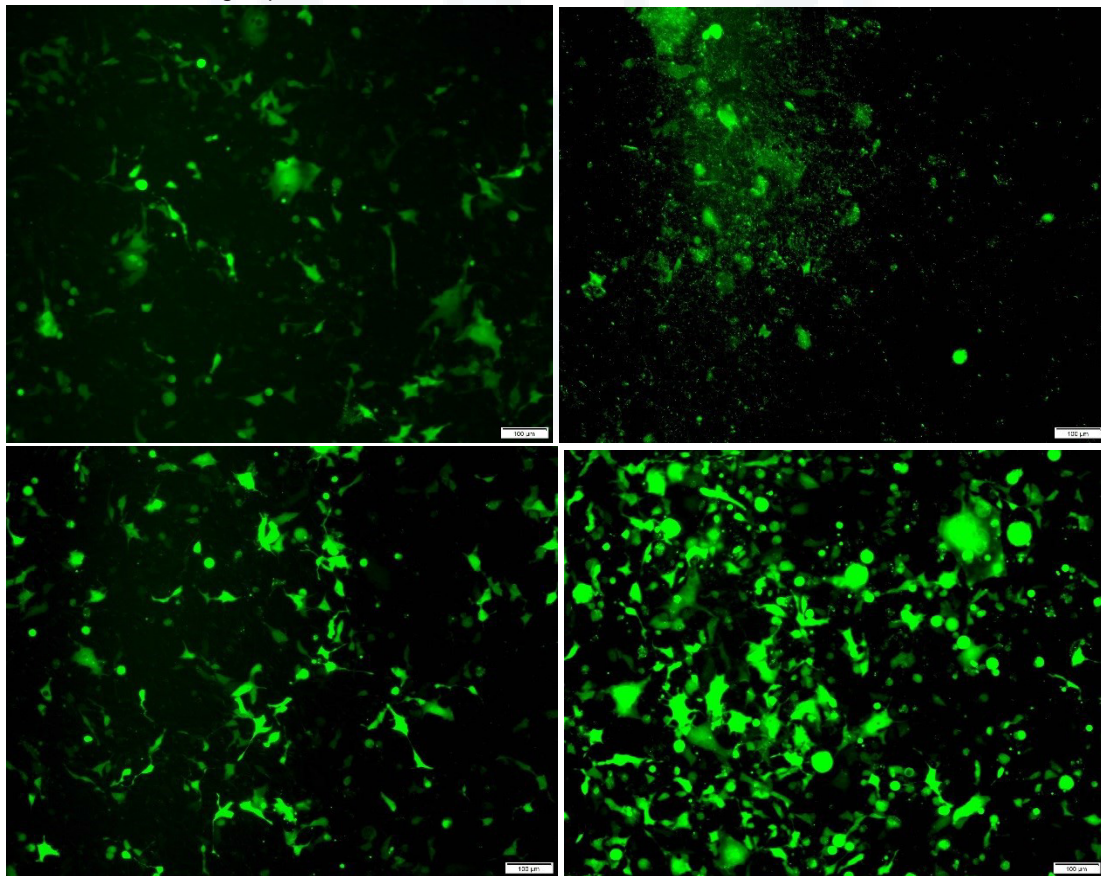


Figure 17: Representative fluorescent images showing the HEK293T cells transduced with either a raw or concentrated GFP-expressing lentivirus. GFP expression was examined 24h (a,c) and 48h (b,d) after transfection, there is an evident increase of luminescence signal. This result confirm the data obtained through PCR technique.

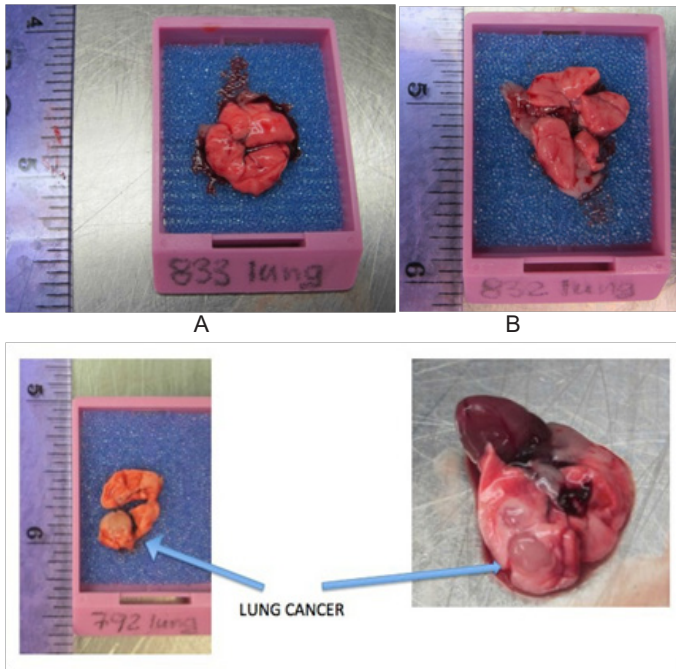


Figure 18: Pictures of lung cancers collected after 4 weeks (A), 8 weeks (B) and 22 weeks (C) Fox Chase Facility did the qualitative and quantitative analysis useful to have the characterization of the different stage or histo types.

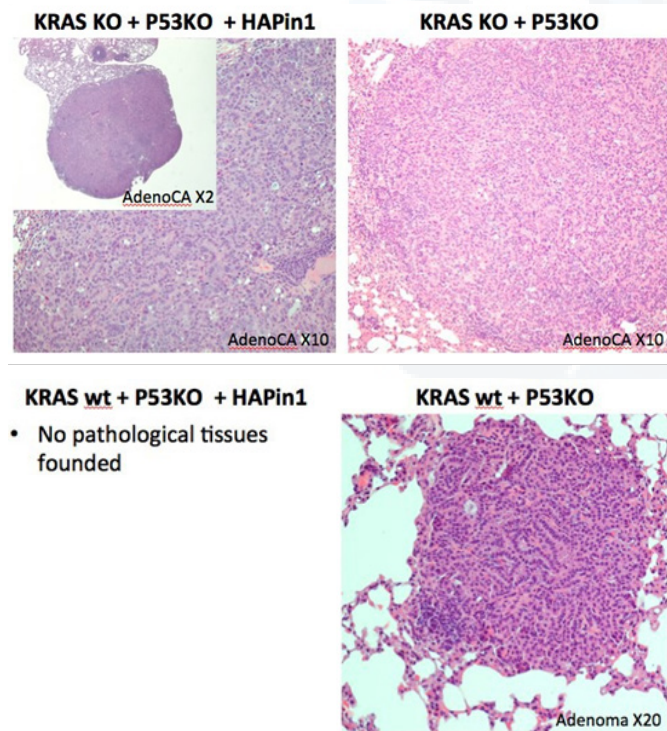


Figure 19: After 22 weeks.

Based on the results obtained considering the incidence of tumor on mice infected with LV carrying pCDH-CRE-HAPin, we can say that where Pin1 is overexpressed we have a more aggressive condition.

Du Page et al. reported also locally metastatic disease to

the mediastinal lymph nodes or the pleural cavity develops in approximately 50% of KP mice as early as 18-20 weeks post- infection. In some mice, distant metastases can be found seeding the liver or the kidneys as early as 20 weeks post-infection. Unfortunately in our study we were not able to find any of these conditions. However, as with most autochthonous mouse tumor models, there is some variation in the results, such as tumor number and approximate time to progression, depending on the strain/ background of mice as well as other factors that vary between institutions, or the efficiency of LV infection after procedure. We have evaluated the recombination of K-rasLSL-G12D and p53fl alleles in tumors by PCR for the presence of a “1 lox”, or recombined, product. Performing PCR on DNA isolated from whole lung after infection to assess infection efficiency confirmed that typically very few cells in the lung have undergone recombination of these alleles, making it difficult to detect it. It is more informative to examine Cre expression after infection by using conditional reporter strains such as Rosa26LSL-LacZ or Rosa26LSL-eGFP and examining reporter expression by immunohistochemistry, immunofluorescence, or fluorescent activated cell sorting. Polyclonal antibodies that can specifically detect the oncogenic K-rasG12D protein are no longer available.

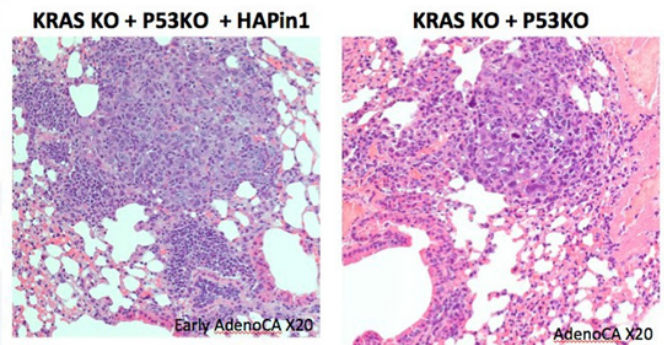


Figure 20: After 16 weeks.

Discussion

Lung cancer is the leading cause of cancer deaths worldwide with non-small cell lung cancer (NSCLC). Progress within the last decade has led to the sophisticated engineering and application of advanced preclinical models of human cancer in the mouse. Several laboratories have constructed genetically-engineered mouse models of NSCLC that mimic the genetic and histopathological features of the human disease. The development of animal models of cancer is critical to our understanding and treatment of the human disease.

Common mutations in NSCLC

- Activating mutations in *K-RAS* (10-30%) plus an oncogenic mutation in *K-RAS* by changing a glycine to aspartic acid at codon 12 in the gene's endogenous locus - To control the expression of K-rasG12D, a lox-stop-lox (LSL) cassette is engineered into the first intron of the *K-ras* gene. The LSL cassette thus creates a

null version of the gene: K-ras null mice are embryonic lethal; therefore, mice can only be heterozygous for the *K-rasLSL-G12D* allele.

- b. Loss of function point mutations in *p53* (50-70%). This 'floxed' *p53* allele (*p53fl*) has LoxP sites flanking exons two through ten of *p53* that are deleted after Cre-mediated recombination, abolishing *p53* function. Prior to Cre-mediated recombination, the *p53* locus is maintained in its wildtype state and *p53* activity is normal.
- c. The activation of oncogenic K-ras along with loss of *p16Ink4a* or *Ink4a/Arf* tumor suppressors, which are mutated in 20-50% of human cases.
- d. Two other subtypes of NSCLC, squamous cell and large cell carcinoma, develop following the combined activation of oncogenic K-ras and loss of the LKB1 tumor suppressor, which is mutant in 10-30% of human cases.
- e. NSCLC models driven by conditionally activated mutations in *Braf* or *EGFR*, mutated in 3% or 10-40% (respectively) of human lung cancers.
- f. A model of small cell lung cancer (SCLC) has been created in which tumors arise following the loss of both the *p53* and *Rb* tumor suppressors [106].

Conditional mouse models provide new opportunities for testing novel chemo preventatives, therapeutics and screening methods that are not possible with cultured cell lines or xenograft models.

Mice model: The time to tumor development vary depending upon the model chosen, and also depend on the amount and type of virus administered to the mice. Increased incidence is due to a greater growth rate of tumors lacking *p53*, leading to rapid development of a tumor that disrupts the normal function of the lungs. In literature is reported that mice infected with 10⁴-10⁵ infectious particles of Lenti-Cre can generate 10-100 tumors per mouse, and we estimate that in our model the number of tumors are still being in the range, considering that we had titrate the virus to 5×10³ infectious particles/mouse. This amount reduces the number of primary tumors and increase the survival time of mice (latency of tumor development), allowing for a greater frequency of metastatic disease in the KP model. Tumors do not always progress in exactly the same way or at the same time; NSCLC model generates a multi-focal disease and therefore we expected some tumor heterogeneity. In this experiment the overexpression of Pin1 in addition to K-ras activation and *p53* loss was expected to impact tumor progression. For that reason, monitoring tumor development and progression histologically was a useful, though difficult, way to follow the disease.

Pin1: Pin1 can be regulated both transcriptionally and post translationally. However, whether *PIN1* is amplified in cancer has not been intensively studied. *PIN1* is a direct target of E2 transcription factor 1 (E2F1), and Her2- and

H-Ras-oncogenic signaling upregulated Pin1 expression via E2F1 [110]. Pin1 activity can also be regulated post-translationally. The binding of Pin1 to its substrates can also be regulated by Pin1 phosphorylation. For instance, 12-O-tetradecanoylphorbol-13- acetate (TPA) treatment results in an interaction between the 90-kDa ribosomal protein S6 kinase 2 and Pin1, leading to the phosphorylation of Pin1 at S16 in the WW domain; this phosphorylation inhibits pSer/Thr-Pro target binding, thus regulating phosphoserine/threonine-binding activity of the WW domain and Pin1 function [111]. In addition, upon forskolin treatment, activated PKA phosphorylates Pin1 at S16 in the WW domain, which results in the removal of Pin1 from nuclear speckles and redistribution of Pin1 throughout the cell. Expression of a mutant Pin1 carrying the WW domain S16A mutation induces mitotic block and apoptosis, and increases multinucleated cells, indicating that Pin1 phosphorylation at S16 has an essential role in cell cycle progression.

Targeting Pin1 for cancer treatment. Compelling data suggest that Pin1 can be targeted to treat human cancer. A number of potent Pin1 antagonists have been developed to either inhibit the PPLase activity of Pin1 or target the Pin1 WW domain to prevent the binding of Pin1 to its substrates [109]. The tumor suppressor *p53* is important in cell cycle arrest or apoptosis in response to a variety of stimuli. In response to DNA damage, *p53* interacts with Pin1, and this interaction is dependent on *p53* phosphorylation. The physiological relationship between Pin1 and *p53* was demonstrated using *Pin1*^{-/-}*p53*^{-/-} mice, which showed that Pin1 ablation inhibited the development of lymphomas in *p53*-deficient mice demonstrating that Pin1 plays an important role in mutant *p53*-promoted transformation and metastasis. In addition, Pin1 promotes the mutant *p53*-dependent inhibition of the anti-metastasis factor *p63* and increase the induction of a mutant *p53* transcriptional activity, which promotes increase tumor aggressiveness. Pin1 also cooperates with mutant *p53* in Ras-dependent transformation to enhance tumorigenesis. Furthermore, in breast cancer patients, the combination of Pin1 overexpression and *p53* mutation is an independent prognostic factor for poor clinical outcome [81]. These results suggest that Pin1 impacts *p53* function at multiple levels [53].

Lentiviral system: Although these Cre/LoxP models provide the most sophisticated means to sporadically control genetic events at their endogenous loci, they are also limited by the difficult requirement to introduce Cre into an initiating cancer cell. The protocol used cannot restrict the genetic events exclusively to initiating cells of the disease because of the inherently non-specific nature of the viruses used to deliver Cre to cells of the lung. However, this has in fact been beneficial in our laboratory because it does not require that investigators identify and target Cre specifically to the cell of origin of the disease. Therefore, despite the drawback of using potentially hazardous viruses, this technique is the most effective means to sporadically deliver Cre specifically

to cells of the lung to initiate lung tumor formation. Although it is possible to perform PCR on DNA isolated from whole lung after infection to assess infection efficiency, this is not recommended and we didn't do that analysis.

Conclusion

Accumulating evidence demonstrates that Pin1 is regulated by different mechanisms at the transcriptional and posttranslational levels and that Pin1 overexpression is correlated with poor prognosis in several types of human cancers. In addition, the Pin1-mediated *cis-trans* isomerization of a wide variety of phosphorylated proteins precisely regulates signal transduction from proteins at the plasma membrane to transcription factors and regulators. Thus, Pin1-mediated *cis-trans* isomerization has profound regulatory effects on many cellular activities, including metabolism, mobility, cell cycle progression, proliferation, survival and apoptosis. The instrumental functions of Pin1 in tumor development make Pin1 a potential target for cancer treatment.

Acknowledgement

None.

Conflict of Interest

No conflict of interest.

References

- Syed Hasan Raza Jafri, Carlos Previgliano, Keerti Khandelwal, Runhua Shi (2015) Cachexia Index in Advanced Non-Small-Cell Lung Cancer Patients. *Clin Med Insights Oncol* 9: 87-93.
- Safari R, Meuwissen R (2015) Practical use of advanced mouse models for lung cancer. *Methods Mol Biol* 1267: 93-124.
- Lemjabbar-Alaoui H, Hassan OU, Yang YW, Buchanan P (2015) Lung cancer: Biology and treatment options. *Biochim Biophys Acta* 1856(2): 189-210.
- Shtivelman E, Hensing T, Simon GR, Dennis PA, Otterson GA, et al. (2014) Molecular pathways and therapeutic targets in lung cancer. *Oncotarget* 5(6): 1392-1433.
- Lynch TJ, Bell DW, Sordella R, Gurubhagavatula S, Okimoto RA, et al. (2004) Activating Mutations in the Epidermal Growth Factor Receptor Underlying Responsiveness of Non-Small-Cell Lung Cancer to Gefitinib. *N Engl J Med* 350(21): 2129-2139.
- Paez JG, Jänne PA, Lee JC, Tracy S, Greulich H, et al. (2004) EGFR Mutations in Lung Cancer: Correlation with Clinical Response to Gefitinib Therapy. *Science* 304(5676): 1497-500.
- Pao W, Miller V, Zakowski M, Doherty J, Politi K, et al. (2004) EGF receptor gene mutations are common in lung cancers from "never smokers" and are associated with sensitivity of tumors to gefitinib and erlotinib. *Proc Natl Acad Sci U S A* 101(36): 13306-13311.
- Pass HI, Carbone, David P, Johnson David H, Minna, John D, et al. (2010) Principles and practice of lung cancer : the official reference text of the IASLC. Lippincott Williams & Wilkins (LWW).
- Hanahan D, Weinberg RA (2011) Hallmarks of Cancer: The Next Generation. *Cell* 144(5): 646-674.
- Dunn GP, Bruce AT, Ikeda H, Old LJ, Schreiber RD, et al. (2002) Cancer immunoediting: from immunosurveillance to tumor escape. *Nat Immunol* 3(11): 991-998.
- Sautès-Fridman C, Cherfils-Vicini J, Damotte D, Fisson S, Fridman WH, et al. (2011) Tumor microenvironment is multifaceted. *Cancer Metastasis Rev* 30(1): 13-25.
- Kerkar SP, Restifo NP (2012) Cellular Constituents of Immune Escape within the Tumor Microenvironment. *Cancer Res* 72(13): 3125-3130.
- De Pas T, Giovannini M, Rescigno M, Catania C, Toffalorio F, Spitaleri G, et al. (2012) Vaccines in non-small cell lung cancer: Rationale, combination strategies and update on clinical trials. *Crit Rev Oncol Hematol* 83(3): 432-443.
- Rodríguez PC, Rodríguez G, González G, Lage A (2010) Clinical development and perspectives of CIMAvax EGF, Cuban vaccine for non-small-cell lung cancer therapy. *MEDICC Rev* 12(1): 17-23.
- Rodriguez E, Mannion L, D'Santos P, Griffiths M, Arends MJ, et al. (2014) Versatile and enhanced tumour modelling in mice via somatic cell transduction. *J Pathol* 232(4): 449-457.
- Sun S, Schiller JH, Gazdar AF (2007) Lung cancer in never smokers-a different disease. *Nat Rev Cancer* 7(10): 778-790.
- DuPage M, Dooley AL, Jacks T (2009) Conditional mouse lung cancer models using adenoviral or lentiviral delivery of Cre recombinase. *Nat Protoc* 4(8): 1064-1072.
- Sylwia Jančík, Jiří Drábek, Danuta Radzioch, Marián Hajdúch (2010) Clinical relevance of KRAS in human cancers. *Journal of biomedicine & biotechnology* 2010: 150960.
- Esser D, Bauer B, Wolthuis RM, Wittinghofer A, Cool RH, et al. (1998) Structure determination of the Ras-binding domain of the Raf-specific guanine nucleotide exchange factor Rf. *Biochemistry* 37(39): 13453-13462.
- Zuber J, Tchernitsa OI, Hinzmann B, Schmitz AC, Grips M, et al. (2000) A genome-wide survey of RAS transformation targets. *Nat Genet* 24(2): 144-152.
- Yanagihara M, Ishikawa S, Naito M, Nakajima J, Aburatani H, et al. (2005) Paired-like homeoprotein ESXR1 acts as a sequence-specific transcriptional repressor of the human K-ras gene. *Oncogene* 24(38): 5878-5887.
- Lagos-Quintana M, Rauhut R, Lendeckel W, Tuschl T (2001) Identification of novel genes coding for small expressed RNAs. *Science* 294(5543): 853-858.
- Anderson MW, Reynolds SH, You M, Maronpot RM (1992) Role of proto-oncogene activation in carcinogenesis. *Environ Health Perspect* 98: 13-24.
- Bos JL, Fearon ER, Hamilton SR, Verlaan-de Vries M, van Boom JH, et al. (1987) Prevalence of ras gene mutations in human colorectal cancers. *Nature* 327(6120): 293-297.
- Schubbert S, Shannon K, Bollag G (2007) Hyperactive Ras in developmental disorders and cancer. *Nature Reviews Cancer* 7(4): 295-308.

26. Jancík S, Drábek J, Radzioch D, Hajdúch M (2010) Clinical relevance of KRAS in human cancers. *J Biomed Biotechnol* 2010: 150960.
27. Scheffzek K, Ahmadian MR, Kabsch W, Wiesmüller L, Lautwein A, et al. (1997) The Ras-RasGAP Complex: Structural Basis for GTPase Activation and Its Loss in Oncogenic Ras Mutants. *Science* 277(5324): 333-338.
28. Serrano M (1997) The Tumor Suppressor Protein p16INK4a. *Exp Cell Res* 237(1): 7-13.
29. Zhang Z, Wang Y, Vikis HG, Johnson L, Liu G, et al. (2001) Wildtype Kras2 can inhibit lung carcinogenesis in mice. *Nature Genetics* 29(1): 25-33.
30. Eberhard DA, Johnson BE, Amler LC, Goddard AD, Heldens SL, et al. (2005) Mutations in the epidermal growth factor receptor and in KRAS are predictive and prognostic indicators in patients with non-small-cell lung cancer treated with chemotherapy alone and in combination with erlotinib. *J Clin Oncol* 23(25): 5900-5909.
31. Riely GJ, Kris MG, Rosenbaum D, Marks J, Li A, et al. (2008) Frequency and distinctive spectrum of KRAS mutations in never smokers with lung adenocarcinoma. *Clin Cancer Res* 14(18): 5731-5734.
32. Sun Y, Ren Y, Fang Z, Li C, Fang R, et al. (2010) Lung adenocarcinoma from East Asian never-smokers is a disease largely defined by targetable oncogenic mutant kinases. *J Clin Oncol* 28(30): 4616-4620.
33. Vogelstein B, Lane D, Levine AJ (2000) Surfing the p53 network. *Nature* 408(6810): 307-310.
34. Jin S, Levine AJ (2001) The p53 functional circuit. *J Cell Sci* 114(Pt23): 4139-4140.
35. Gudkov AV, Komarova EA (2003) The role of p53 in determining sensitivity to radiotherapy. *Nature reviews. Cancer* 3(2): 117-129.
36. Oren M (2003) Decision making by p53: life, death and cancer. *Cell death and differentiation* 10(4): 431-442.
37. Appella E, Anderson CW (2001) Post-translational modifications and activation of p53 by genotoxic stresses. *Eur J Biochem FEBS* 268(10): 2764-2772.
38. Lowe SW, Sherr CJ (2003) Tumor suppression by Ink4a-Arf: progress and puzzles. *Curr Opin Genet Dev* 13(1): 77-83.
39. Harris SL, Levine AJ (2005) The p53 pathway: positive and negative feedback loops. *Oncogene* 24(17): 2899-2908.
40. Haupt Y, Rowan S, Shaulian E, Kazaz A, Vousden K, et al. (1997) p53 mediated apoptosis in HeLa cells: transcription dependent and independent mechanisms. *Leukemia* 11(Suppl 3): 337-339.
41. Blandino G, Levine AJ, Oren M (1999) Mutant p53 gain of function: differential effects of different p53 mutants on resistance of cultured cells to chemotherapy. *Oncogene* 18(2): 477-85.
42. de Vries A, Flores ER, Miranda B, Hsieh HM, van Oostrom CT, et al. (2002) Targeted point mutations of p53 lead to dominant-negative inhibition of wild-type p53 function. *Proc Natl Acad Sci U S A* 99(5): 2948-2953.
43. Blume-Jensen P, Hunter T (2001) Oncogenic kinase signalling. *Nature* 411(6835): 355-365.
44. Pawson T, Scott JD (2005) Protein phosphorylation in signaling--50 years and counting. *Trends Biochem Sci* 30(6): 286-290.
45. Lee TH, Pastorino L, Lu KP (2011) Peptidyl-prolyl cis-trans isomerizes Pin1 in ageing, cancer and Alzheimer disease. *Expert Rev Mol Med* 13(6835): e21.
46. Göthel S, Marahiel MA (1999) Peptidyl-prolyl cis-trans isomerizes a super family of ubiquitous folding catalysts. *Cell Mol Life Sci* 55(3): 423-436.
47. Lu KP, Hanes SD, Hunter T (1996) A human peptidyl-prolyl isomerizes essential for regulation of mitosis. *Nature* 380(6574): 544-547.
48. Ranganathan R, Lu KP, Hunter T, Noel JP (1997). Structural and functional analysis of the mitotic rotamase Pin1 suggests substrate recognition is phosphorylation dependent. *Cell* 89(6): 875-886.
49. Fischer G, Aumüller T (2003) Regulation of peptide bond cis/trans isomerization by enzyme catalysis and its implication in physiological processes. *Reviews of physiology, biochemistry and pharmacology* 148: 105-150.
50. Werner-Allen JW, Lee CJ, Liu P, Nicely NI, Wang S, et al. (2011) Cis-Proline-mediated Ser (P)5 dephosphorylation by the RNA polymerase II C-terminal domain phosphatase Ssu72. *The Journal of biological chemistry* 286(7): 5717-5726.
51. Suizu F, Ryo A, Wulf G, Lim J, Lu KP (2006) Pin1 regulates centrosome duplication, and its overexpression induces centrosome amplification, chromosome instability, and oncogenesis. *Molecular and cellular biology* 26(4): 1463-1479.
52. Wulf G, Garg P, Liou YC, Iglehart D, Lu KP (2004) Modeling breast cancer in vivo and ex vivo reveals an essential role of Pin1 in tumorigenesis. *The EMBO Journal* 23(16): 3397-3407.
53. Takahashi K, Akiyama H, Shimazaki K, Uchida C, Akiyama-Okunuki H, Tomita M, et al. (2007) Ablation of a peptidyl prolyl isomerase Pin1 from p53-null mice accelerated thymic hyperplasia by increasing the level of the intracellular form of Notch1. *Oncogene* 26(26): 3835-3845.
54. Bao L, Kimzey A, Sauter G, Sowadski JM, Lu KP, et al. (2004) Prevalent overexpression of prolyl isomerase Pin1 in human cancers. *Am J Pathol* 164(5): 1727-1737.
55. Tan X, Zhou F, Wan J, Hang J, Chen Z, et al. (2010) Pin1 expression contributes to lung cancer: Prognosis and carcinogenesis. *Cancer Biol Ther* 9(2): 111-119.
56. Leung KW, Tsai CH, Hsiao M, Tseng CJ, Ger LP, et al. (2009) Pin1 overexpression is associated with poor differentiation and survival in oral squamous cell carcinoma. *Oncology reports* 21(4): 1097-1104.
57. Lee TH, Chen CH, Suizu F, Huang P, Schiene Fischer C, et al. (2011) Death-associated protein kinase 1 phosphorylates Pin1 and inhibits its prolyl isomerase activity and cellular function. *Mol Cell* 42(2): 147-59.
58. Rangasamy V, Mishra R, Sondarva G, Das S, Lee TH, et al. (2012) Mixed-lineage kinase 3 phosphorylates prolyl-isomerase Pin1 to regulate its nuclear translocation and cellular function. *Proc Natl Acad Sci U S A* 109(21): 8149-8154.

59. Eckerdt F, Yuan J, Saxena K, Martin B, Kappel S, et al. (2005) Polo-like kinase 1-mediated phosphorylation stabilizes Pin1 by inhibiting its ubiquitination in human cells. *J Biol Chem* 280(44): 36575-3683.
60. Chen CH, Chang CC, Lee TH, Luo M, Huang P, et al. (2013) SENP1 deSUMOylates and regulates Pin1 protein activity and cellular function. *Cancer research* 73(13): 3951-3962.
61. Lu Z, Hunter T (2009) Degradation of activated protein kinases by ubiquitination. *Annu Rev Biochem* 78: 435-475.
62. Penela P, Rivas V, Salcedo A, Mayor F (2010) G protein-coupled receptor kinase 2 (GRK2) modulation and cell cycle progression. *Proc Natl Acad Sci U S A* 107(3): 1118-1123.
63. Wells NJ, Watanabe N, Tokusumi T, Jiang W, Verdecia MA, et al. (1999) The C-terminal domain of the Cdc2 inhibitory kinase Myt1 interacts with Cdc2 complexes and is required for inhibition of G(2)/M progression. *J Cell Sci* 3361-3371.
64. Crenshaw DG, Yang J, Means AR, Kornbluth S (1998) The mitotic peptidyl-prolyl isomerase, Pin1, interacts with Cdc25 and Plx1. *EMBO J* 17(5): 1315-1327.
65. Stukenberg PT, Kirschner MW (2001) Pin1 acts catalytically to promote a conformational change in Cdc25. *Mol cell* 7(5): 1071-1083.
66. Liou YC, Ryo A, Huang HK, Lu PJ, Bronson R et al. (2002) Loss of Pin1 function in the mouse causes phenotypes resembling cyclic D1- null phenotypes. *Proc Natl Acad Sci U S A* 99(3): 1335-1340.
67. Diehl JA, Cheng M, Roussel MF, Sherr CJ (1998) Glycogen synthase kinase-3beta regulates cyclic D1 proteolysis and subcellular localization. *Genes Dev* 12(22): 3499-3511.
68. Yeh ES, Lew BO, Means AR (2006) The loss of PIN1 deregulates cyclic E and sensitizes mouse embryo fibroblasts to genomic instability. *J Biol Chem* 281(1): 241-251.
69. Minella AC, Welcker M, Clurman BE (2005) Ras activity regulates cyclic E degradation by the Fbw7 pathway. *Proc Natl Acad Sci U S A* 102(27): 9649-9654.
70. Wierød L, Rosseland CM, Lindeman B, Oksvold MP, Grøsvik H, et al. (2007) CDK2 regulation through PI3K and CDK4 is necessary for cell cycle progression of primary rat hepatocytes. *Cell Prolif* 40(4): 475-487.
71. Lucchetti C, Caligiuri I, Toffoli G, Giordano A, Rizzolio F (2013) The prolyl isomerase Pin1 acts synergistically with CDK2 to regulate the basal activity of estrogen receptor α in breast cancer. *PLoS One* 8(2): 55355e.
72. Lannigan DA (2003) Estrogen receptor phosphorylation. *Steroids* 68(1): 1-9.
73. Rajbhandari P, Finn G, Solodin NM, Singarapu KK, Sahu SC et al. (2012) Regulation of estrogen receptor α N-terminus conformation and function by peptidyl prolyl isomerase Pin1. *Mol Cell Biol* 32(2): 445-457.
74. Rajbhandari P, Schalper KA, Solodin NM, Ellison-Zelski SJ, Ping Lu K, et al. (2014) Pin1 modulates ER α levels in breast cancer through inhibition of phosphorylation-dependent ubiquitination and degradation. *Oncogene* 33(11): 1438-1447.
75. Yi P, Wu RC, Sandquist J, Wong J, Tsai SY, et al. (2005) Peptidyl-prolyl isomerase 1 (Pin1) serves as a coactivator of steroid receptor by regulating the activity of phosphorylated steroid receptor coactivator 3 (SRC-3/AIB1). *Mol Cell Biol* 25(21): 9687-9699.
76. Lee TH, Pastorino L, Kun Ping Lu (2011) Peptidyl-prolyl cis-trans isomerase Pin1 in ageing, cancer and Alzheimer disease. *Expert Reviews in Molecular Medicine* 13(6835): p.e21.
77. Rizzolio F, Lucchetti C, Caligiuri I, Marchesi I, Caputo M et al. (2012) Retinoblastoma tumor-suppressor protein phosphorylation and inactivation depend on direct interaction with Pin1. *Cell Death Differ* 19(7): 1152-1161.
78. Zheng H, You H, Zhou XZ, Murray SA, Uchida T et al. (2002) The prolyl isomerase Pin1 is a regulator of p53 in genotoxic response. *Nature* 419(6909): 849-853.
79. Paola Zacchi, Monica Gostissa, Takafumi Uchida, Clio Salvagno, Fabio Avolio, et al. (2002) The prolyl isomerase Pin1 reveals a mechanism to control p53 functions after genotoxic insults. *Nature* 419(6909): 853-857.
80. Wulf GM, Liou YC, Ryo A, Lee SW, Lu KP (2002) Role of Pin1 in the regulation of p53 stability and p21 transactivation, and cell cycle checkpoints in response to DNA damage. *J Biol Chem* 277(50): 47976-47979.
81. Girardini JE, Napoli M, Piazza S, Rustighi A, Marotta C et al. (2011) A Pin1/mutant p53 axis promotes aggressiveness in breast cancer. *Cancer cell* 20(1): 79-91.
82. Peter Manilla, Tessio Rebello, Cathleen Afable, Xiaobin Lu, Vladimir Slepishkin, et al. (2005) Regulatory Considerations for Novel Gene Therapy Products: A Review of the Process Leading to the First Clinical Lentiviral Vector. *Human Gene Therapy* 16(1): 17-25.
83. Sutton RE, Reitsma MJ, Uchida N, Brown PO (1999) Transduction of human progenitor hematopoietic stem cells by human immunodeficiency virus type 1-based vectors is cell cycle dependent. *J Virol* 73(5): 3649-3660.
84. Gally, P. et al., 1995. HIV nuclear import is governed by the phosphotyrosine-mediated binding of matrix to the core domain of integrase. *Cell*, 83(4), pp.569-576.
85. Carlos MC de Noronha, Michael P Sherman, Harrison W Lin, Marielle V Cavois, Robert D Moir, et al. (2001) Dynamic Disruptions in Nuclear Envelope Architecture and Integrity Induced by HIV-1 Vpr. *Science* 294(5544): 1105-1108.
86. Brenner S, Malech HL (2003) Current developments in the design of onco-retrovirus and lentivirus vector systems for hematopoietic cell gene therapy. *Biochimica et Biophysica Acta (BBA)-Molecular Cell Research* 1640(1): 1-24.
87. Cooray S, Howe SJ, Thrasher AJ (2012) Chapter three- Retrovirus and Lentivirus Vector Design and Methods of Cell Conditioning. In *Methods in Enzymology* 507: 29-57.
88. Trono D (2000) Lentiviral vectors: turning a deadly foe into a therapeutic agent. *Gene Therapy* 7(1): 20-23.
89. S Charrier, L Dupré, S Scaramuzza, L Jeanson-Leh, M P Blundell, et al. (2007) Lentiviral vectors targeting WASp expression to hematopoietic cells, efficiently transduce and correct cells from WAS patients. *Gene Therapy* 14(5): 415-428.
90. de Seranno S, Meuwissen R (2010) Progress and applications of mouse models for human lung cancer. *The Eur Respir J* 35(2): 426-443.

91. Jacks T (1992) Effects of an Rb mutation in the mouse. *Nature* 359(6393): 295-300.
92. Singer O, Verma IM (2008) Applications of lentiviral vectors for shRNA delivery and Trans genesis. *Curr Gene Ther* 8(6): 483-488.
93. Breyer B, Jiang W, Cheng H, Zhou L, Paul R, et al. (2001) Adenoviral vector-mediated gene transfer for human gene therapy. *Curr Gene Ther* 1(2): 149-162.
94. Winslow MM, Dayton TL, Verhaak RG, Kim-Kiselak C, Snyder EL, et al. (2011) Suppression of lung adenocarcinoma progression by Nkx2-1. *Nature* 473(7345): 101-104.
95. Hameyer D, Loonstra A, Eshkind L, Schmitt S, Antunes C, et al. (2007) Toxicity of ligand-dependent Cre recombinase and generation of a conditional Cre delete mouse allowing mosaic recombination in peripheral tissues. *Physiol Genomics* 31(1): 32-41.
96. Pfeifer A, Brandon EP, Kootstra N, Gage FH, Verma IM, et al. (2001) Delivery of the Cre recombinase by a self-deleting lentiviral vector: efficient gene targeting in vivo. *Proc Natl Acad Sci U S A* 98(20): 11450-11455.
97. Rodriguez E (2014) Versatile and enhanced tumour modeling in mice via somatic cell transduction. *The Journal of Pathology* 232(4): 449-457.
98. Lu PJ, Zhou XZ, Liou YC, Noel JP, Lu KP, et al. (2002) Critical role of WW domain phosphorylation in regulating phosphoserine binding activity and Pin1 function. *J Biol Chem* 277(4): 2381-2384.
99. Olive KP, Tuveson DA, Ruhe ZC, Yin B, Willis NA, et al. (2004) Mutant p53 gain of function in two mouse models of Li-Fraumeni syndrome. *Cell* 119(6): 847-860.
100. Smith AJ, Xian J, Richardson M, Johnstone KA, Rabbitts PH, et al. (2002) Cre-loxP chromosome engineering of a targeted deletion in the mouse corresponding to the 3p21.3 region of homozygous loss in human tumours. *Oncogene* 21(29): 4521-4529.
101. Meuwissen R, Linn SC, van der Valk M, Mooi WJ, Berns A, et al. (2001) Mouse model for lung tumorigenesis through Cre/lox controlled sporadic activation of the K-Ras oncogene. *Oncogene* 20(45): 6551-6558.
102. Tichelaar JW, Lu W, Whitsett JA (2000) Conditional expression of fibroblast growth factor-7 in the developing and mature lung. *J Biol Chem* 275(16): 11858-11864.
103. Kwon MC, Berns A (2013) Mouse models for lung cancer. *Mol Oncol* 7(2): 165-177.
104. Floyd HS, Farnsworth CL, Kock ND, Mizesko MC, Little JL, et al. (2005) Conditional expression of the mutant Ki-rasG12C allele results in formation of benign lung adenomas: development of a novel mouse lung tumor model. *Carcinogenesis* 26(12): 2196-2206.
105. Sweet-Cordero A, Mukherjee S, Subramanian A, You H, Roix JJ, et al. (2005) An oncogenic KRAS2 expression signature identified by cross-species gene-expression analysis. *Nat Genet* 37(1): 48-55.
106. Meuwissen R, Linn SC, Linnoila RI, Zevenhoven J, Mooi WJ, et al. (2003) Induction of small cell lung cancer by somatic inactivation of both Trp53 and Rb1 in a conditional mouse model. *Cancer cell* 4(3): 181-189.
107. van den Heuvel S, Harlow E (1993) Distinct roles for cyclic-dependent kinases in cell cycle control. *Science* 262(5142): 2050-2054.
108. Malumbres M, Barbacid M (2009) Cell cycle, CDKs and cancer: a changing paradigm. *Nature Reviews Cancer* 9(3): 153-166.
109. Moore JD, Potter A (2013) Pin1 inhibitors: Pitfalls, progress and cellular pharmacology. *Bioorg Med Chem Lett* 23(15): 4283-4291.
110. Ryo A, Liou YC, Wulf G, Nakamura M, Lee SW, et al. (2002) PIN1 is an E2F target gene essential for Neu/Ras-induced transformation of mammary epithelial cells. *Mol Cell Biol* 22(15): 5281-9525.
111. Lu KP, Zhou XZ (2007) The prolyl isomerizes PIN1: a pivotal new twist in phosphorylation signalling and disease. *Nat Rev Mol Cell Biol* 8(11): 904-916.
112. Dornan D, Wertz I, Shimizu H, Arnott D, Frantz GD, et al. (2004) The ubiquitin ligase COP1 is a critical negative regulator of p53. *Nature* 429(6987): 86-92.
113. Harms K, Nozell S, Chen X (2004) The common and distinct target genes of the p53 family transcription factors. *Cell Mol Life Sci* 61(7-8): 822-42.
114. Leng RP, Lin Y, Ma W, Wu H, Lemmers B, et al. (2003) Pirh2, a p53-induced ubiquitin-protein ligase, promotes p53 degradation. *Cell* 112(6): 779-791.
115. Takekawa M, Adachi M, Nakahata A, Nakayama I, Itoh F, et al. (2000) p53-inducible wip1 phosphatase mediates a negative feedback regulation of p38 MAPK-p53 signaling in response to UV radiation. *The EMBO journal* 19(23): 6517-6526.
116. The Jacks Lab, DNA Isolation from Tails - Proteinase K Method | Jacks Lab.
117. Simon Swingler, Jinping Song, Frederic Bushman, Didier Trono (1995) HIV nuclear import is governed by the phosphotyrosine-mediated binding of matrix to the core domain of integrase. *Cell* 83(4): 569-576.